

**NEWLY RESOLVED RELATIONSHIPS IN AN EARLY LAND PLANT  
 LINEAGE: BRYOPHYTA CLASS SPHAGNOPSIDA (PEAT MOSSES)<sup>1</sup>**

A. JONATHAN SHAW<sup>2,11</sup>, CYMON J. COX<sup>3</sup>, WILLIAM R. BUCK<sup>4</sup>, NICOLAS DEVOS<sup>5</sup>, ALEX M. BUCHANAN<sup>6</sup>, LYNETTE CAVE<sup>6</sup>, RODNEY SEPPELT<sup>7</sup>, BLANKA SHAW<sup>2</sup>, JUAN LARRAÍN<sup>8</sup>, RICHARD ANDRUS<sup>9</sup>, JOHANN GREILHUBER<sup>10</sup>, AND EVA M. TEMSCH<sup>10</sup>

<sup>2</sup>Duke University, Department of Biology, Durham, North Carolina 27708 USA; <sup>3</sup>Centro de Ciências do Mar, Universidade do Algarve, Campus de Gambelas, 8005-139 Faro, Portugal; <sup>4</sup>Institute of Systematic Botany, The New York Botanical Garden, Bronx, New York 10458 USA; <sup>5</sup>Institute of Botany, University of Liège, B22 Sart Tilman, B-4000 Liège, Belgium; <sup>6</sup>Tasmanian Herbarium, Private Bag 4, Hobart, Tasmania 7001, Australia; <sup>7</sup>Australian Antarctic Division, Channel Highway, Kingston, Tasmania 7050, Australia; <sup>8</sup>Departamento de Botánica, Universidad de Concepción, Casilla 160-C, Concepción, Chile; <sup>9</sup>Departments of Environmental Studies and Biological Sciences, Binghamton University, Vestal Parkway East, P.O. Box 6000, Binghamton, New York 13902 USA; and <sup>10</sup>Department of Systematic and Evolutionary Botany, Faculty of Life Sciences, University of Vienna, Rennweg 14, A 1030 Vienna, Austria

- *Premise of the study:* The Sphagnopsida, an early-diverging lineage of mosses (phylum Bryophyta), are morphologically and ecologically unique and have profound impacts on global climate. The Sphagnopsida are currently classified in two genera, *Sphagnum* (peat mosses) with some 350–500 species and *Ambuchanania* with one species. An analysis of phylogenetic relationships among species and genera in the Sphagnopsida were conducted to resolve major lineages and relationships among species within the Sphagnopsida.
- *Methods:* Phylogenetic analyses of nucleotide sequences from the nuclear, plastid, and mitochondrial genomes (11 704 nucleotides total) were conducted and analyzed using maximum likelihood and Bayesian inference employing seven different substitution models of varying complexity.
- *Key results:* Phylogenetic analyses resolved three lineages within the Sphagnopsida: (1) *Sphagnum sericeum*, (2) *S. inretortum* plus *Ambuchanania leucobryoides*, and (3) all remaining species of *Sphagnum*. Sister group relationships among these three clades could not be resolved, but the phylogenetic results indicate that the highly divergent morphology of *A. leucobryoides* is derived within the Sphagnopsida rather than plesiomorphic. A new classification is proposed for class Sphagnopsida, with one order (Sphagnales), three families, and four genera.
- *Conclusions:* The Sphagnopsida are an old lineage within the phylum Bryophyta, but the extant species of *Sphagnum* represent a relatively recent radiation. It is likely that additional species critical to understanding the evolution of peat mosses await discovery, especially in the southern hemisphere.

**Key words:** *Ambuchanania*; bryophyte phylogeny; land plant phylogeny; peat mosses; Sphagnopsida; *Sphagnum*.

Phylogenetic analyses of genome structure and nucleotide sequences from mitochondrial, plastid, and nuclear genes have corroborated the view held by botanists for over a century that the bryophyte groups (mosses, liverworts, hornworts) comprise early-diverging land plant lineages that originated before the appearance of vascular plants (Haeckel, 1876; Campbell, 1895; Bower, 1935; Kenrick and Crane, 1997; Shaw and Renzaglia, 2004). Early cladistic analyses based on morphological characters (Mishler and Churchill, 1984) showed that the three bryophyte groups, classified by most botanists of the time as a single phylum because of their similar gametophyte-dominant life cycles, more likely represent a paraphyletic grade that diverged before the emergence of the vascular plants. In fact, Haeckel's

(1876) tree similarly shows mosses and liverworts as a paraphyletic grade basal to the vascular plants. Recent data sets appear to favor the hypothesis that liverworts (phylum Marchantiophyta) comprise the earliest-diverging lineage, followed by the mosses (Bryophyta) and hornworts (Anthoceroophyta) (Qiu et al., 1998; Nickrent et al., 2000; Shaw and Renzaglia, 2004). However, the most data-rich studies to date, based on chloroplast or mitochondrial organellar proteins, like analyses based on sperm cell morphology (Garbary et al., 1993), identify a clade uniting liverworts and mosses, and additional data are still needed before we can consider the branching order of early land plant lineages to be finally resolved (Nishiyama et al., 2004; Rodríguez-Ezpeleta et al., 2007; Terasawa et al., 2007; but see also Qiu, et al., 2006).

Notwithstanding that much remains to do, great progress has been made toward resolving phylogenetic relationships within the mosses (phylum Bryophyta s.s.) (e.g., Cox and Hedderson, 1999; Cox et al., 2000; Newton et al., 2000; Goffinet et al., 2001; Stech and Frey, 2008; Goffinet et al., 2009; Wahrmond et al., 2010). Major clades resolved by molecular data to a large extent mirror previous classifications based on morphology (e.g., Fleischer, 1923; Brotherus, 1924–1925; Vitt, 1984). A simple classification for Bryophyta that represents phylogenetic relationships divides the phylum into five classes: Bryopsida,

<sup>1</sup> Manuscript received 10 February 2010; revision accepted 16 June 2010.

This research was supported NSF grant no. DEB-0918998 to A.J.S. and B.S. The authors thank Sandra Boles, Duke University, for technical assistance and Robert Krisai, University of Salzburg, for providing a herbarium specimen of *Sphagnum girgensohnii* from the Lesachtal, Lungau, Salzburg for genome size analysis.

<sup>11</sup> Author for correspondence (e-mail: shaw@duke.edu)

Takakiopsida, Andreaeopsida, Andreaebryopsida, and Sphagnopsida (Stech and Frey, 2008; Goffinet et al., 2009). The classes of phylum Bryophyta differ in basic developmental features including embryological origins of the sporogenous and columellar tissue of sporophytes, dehiscence of sporangia, and morphology of the gametangia and sperm cells (Cavers, 1911; Schofield, 1985; Crum, 2001b; Garbary et al., 1993; Vanderpoorten and Goffinet, 2009). The class Bryopsida includes most familiar mosses, with some 10 000 species (Crosby et al., 2000). The Andreaeopsida and Sphagnopsida each include about 350–500 species, the Takakiopsida two, and Andreaebryopsida one.

The Sphagnopsida comprise a morphologically distinctive group, and some have argued that they should be classified in a phylum separate from other mosses (Steere, 1958; Crum, 2001b). Phylogenetic analyses based on morphological and molecular characters, however, have shown that the Sphagnopsida are part of a monophyletic Bryophyta (i.e., mosses: Garbary et al., 1993; Hedderson et al., 1996; Beckert et al., 1999). Within the Bryophyta, plants of Sphagnopsida are distinguished from other mosses by numerous morphological and developmental features. Gametophyte features include thalloid protonemata (shared with Andreaeopsida and a few early-diverging members of the Bryopsida), dimorphic leaf cells of mature leaves, and typical absence of rhizoids attaching mature plants to their substrates. Enlarged, hyaline leaf cells, dead at maturity and with various reinforcing cell wall fibrils and pores, are enclosed within a network of much narrower chlorophyllose cells. This pattern is not found in any other moss, although loosely analogous cell dimorphism occurs in scattered species of the class Bryopsida. Ontogeny of the chlorophyllose and hyaline cells during leaf development in *Sphagnum* is unique (e.g., Holcombe, 1984; Butterfass, 1992). Asymmetric cell divisions during leaf ontogeny give rise to groups of three cells from a single initial (a so-called triad), one hyaline and empty at maturity and two chlorophyllose cells (Butterfass, 1992). At maturity, each hyaline cell is surrounded by five or more narrow hyaline cells, two of them derived from the same triad and others related by cell lineage to adjacent hyaline cells.

The Sphagnopsida also differ from other mosses in that elongation of gametophyte stems involves subapical meristematic activity in fully differentiated cells derived from the apical cell itself (Ligrone and Duckett, 1998). The sperm cells of *Sphagnum* are characterized by at least five apomorphic character states pertaining to the flagellar apparatus, and antheridia of *Sphagnum* differ from those in other mosses in lacking opercular cells (Garbary et al., 1993). The gametophyte–sporophyte junction in *Sphagnum* lacks placental wall ingrowths, in contrast to those of other mosses (Ligrone et al., 1993).

The sporophyte generation of Sphagnopsida is also highly differentiated. The sporophyte lacks a seta (stalk) and is instead raised on a pseudopodium of (maternal) gametophyte origin, a feature shared with Andreaeopsida but not Andreaebryopsida, Bryopsida, or Takakiopsida. The sporogenous tissue within the sporangium of Sphagnopsida develops from embryonic amphithecium rather than endothelial tissue and overarches a massive columella (derived from the endothecium). The columella is much more slender in other mosses and the sporogenous tissue is derived from the outer layer(s) of endothecium, rather than the amphithecium. Endothecium and amphithecium differentiate at a very early stage of sporophyte development, and the difference between Sphagnopsida and other mosses is viewed as fundamental. The sporangia (capsules) of Sphagnopsida dehisce by an apical operculum, as in Bryopsida (in contrast to the vertical or spiral suture lines in Andreaeopsida/Andreaebryopsida

and Takakiopsida, respectively), but unlike most true mosses (Bryopsida), Sphagnopsida have no peristomes and the capsules open via a unique “pop-gun” mechanism wherein the operculum detaches explosively as the capsule shrinks in diameter (Duckett et al., 2009).

The Sphagnopsida are currently classified in two orders (Ambuchananiales, Sphagnales), each with a single family and genus (Ambuchananiaceae, *Ambuchanania*; Sphagnaceae, *Sphagnum*) (Seppelt, 2000; Crum, 2001b). *Ambuchanania leucobryoides* (as *Sphagnum*) was described (Yamaguchi et al., 1990) from a single collection made in Tasmania in 1987. It was first classified in a new section of *Sphagnum* but later (Crum and Seppelt, 1999) moved to a newly erected family and order.

*Ambuchanania* has hyaline and chlorophyllose (i.e., dimorphic) leaf cells like *Sphagnum*, and some of the hyaline cells are ornamented with cell wall fibrils and pores. Although the morphological details of the leaf areolation differ from any *Sphagnum* species, these features clearly connect *Ambuchanania* to the latter genus. Also like *Sphagnum*, *Ambuchanania* gametophytes lack rhizoids at maturity. Gametophyte plants are relatively small and lack fasciculate branching, an unusual but not unique trait in *Sphagnum*. *Ambuchanania* has bisexual gametophytes like some species of *Sphagnum*, but the antheridia are oblong-elongate, unlike the spherical antheridia of *Sphagnum*. The antheridia of *Ambuchanania* occur in naked clusters below the archegonia, rather than on well-differentiated branches as in *Sphagnum*, and the archegonia are terminal on stems rather than on short lateral branches as in *Sphagnum*.

The sporophyte of *Ambuchanania* is similar to those in *Sphagnum* and is raised on a terminal pseudopodium of gametophytic origin. Like *Sphagnum*, the capsule wall of *Ambuchanania* has abundant pseudostomata, similar in structure to stomata but apparently nonfunctional (Crum, 2001b; Duckett et al., 2009).

It is because of these many structural features that distinguish *Ambuchanania* from *Sphagnum* that the genus has been classified in a separate family and order from *Sphagnum*. This interpretation is supported by molecular phylogenetic data presented by Shaw (2000) and greatly expanded here. The interpretation of morphological evolution in the Sphagnopsida and the classification for the group are, however, complicated by new information (below) that several species having more or less typical morphology for *Sphagnum* are more closely related to *Ambuchanania* than they are to *Sphagnum* s.s.

In this paper, we present new molecular data on relationships in the Sphagnopsida, illustrate selected morphological characters of *Ambuchanania* and related species, and propose a new classification for the class Sphagnopsida.

## MATERIALS AND METHODS

**Taxon sampling and data acquisition**—Extraction, amplification, and sequencing followed protocols described in Shaw et al. (2003). The following genes were sequenced: photosystem II (PSII) reaction center protein D1 (*psbA*), photosystem II (PSII) reaction center protein T (*psbT-H*), ribulose-bisphosphate carboxylase gene (*rbcL*), RNA polymerase subunit beta (*rpoC1*), ribosomal small protein 4 (*rps4*), tRNA(Gly) (UCC) (*trnG*), and the *trnL* (UAA) 59 exon-*trnF* (GAA) region (*trnL*) from the plastid genome; introns within NADH protein-coding subunits 5 and 7 (*nad5*, *nad7*, respectively) from the mitochondrial genome; and 18S ribosomal RNA (18S) and 26S ribosomal RNA (26S) from the nuclear genome. The nuclear ribosomal internal transcribed spacer region (ITS) was sequenced in selected species and inferences from these data are briefly discussed, but they were not included in the formal phylogenetic analyses. Primer sequences for amplifying and sequencing the loci were provided in Shaw et al. (2003), with the exception of *rpoC1*. For this locus, we used primers

described in the Royal Botanic Gardens, Kew, web page: DNA Barcoding, phase 2 protocols (<http://www.kew.org/barcoding/protocols.html>).

Two multilocus molecular data sets were constructed, one with a diverse range of 56 taxa drawn from across the Bryophyta plus four species of Marchantiophyta as outgroups (60 taxa and eight loci), and a second data set with a restricted number of taxa but more data (nine taxa and 11 loci). The 60-taxon data set includes 26 species of class Bryopsida, the “true” (peristomate) mosses. These represent all major clades of Bryopsida; the data set was used by Cox et al. (2004) to resolve backbone relationships among mosses. As in that previous analysis (Cox et al., 2004), our data set also includes (in addition to Bryopsida) one sample each of *Takakia* (Takakiopsida), *Andreaea* (Andreaeopsida), and *Andreaobryum* (Andreaobryopsida). To this data set we added 24 species of *Sphagnum* representing all the commonly recognized infrageneric groups (subgenera or sections, depending on the author; e.g., Warnstorff, 1911; Crum, 1984), plus two species of uncertain relationship within *Sphagnum* (i.e., *S. sericeum* Müll. Hal., *S. inretortum* H. A. Crum; Shaw et al., 2003 [the latter as *S. lapazense*]), and a sample of *Ambuchanania leucobryoides* recently collected from Tasmania (Johnson et al., 2008).

In an attempt to evaluate the possibility that *Ambuchanania leucobryoides* and *S. inretortum* are sister species, a hypothesis developed from analyses of the 60-taxon data set, we removed the liverwort outgroups and all exemplars of class Bryopsida, represented *Sphagnum* s.s. (which is unambiguously supported as monophyletic) by two divergent species, and also included *Ambuchanania*, *S. inretortum* and *S. sericeum*, which were resolved outside *Sphagnum* s.s. in the 60-taxon analysis (as well as by analyses in Shaw et al., 2003). Exemplars of *Andreaea* and *Takakia* were included as outgroups to establish phylogenetic polarity within the Sphagnopsida.

One of the critical taxa in this study, *S. inretortum*, is represented by two population samples in our analyses. One is the type specimen of *S. lapazense* H. A. Crum (Bolivia, sampled with permission of H. Crum), and the second is from a morphologically similar population (Chile) discovered while this work was in progress. When this manuscript was almost completed, we realized (based on morphological comparisons) that the type specimen of *S. inretortum* (Bolivia) also appears to be conspecific with plants from these other populations. The type of *S. inretortum* was collected in 1981 and attempts to amplify DNA from it (with permission of H. Crum) have been unsuccessful. On the basis of morphological similarities all three specimens are referred to here as *S. inretortum*, which is an earlier name than *S. lapazense*.

Reduced sampling relative to the 60-taxon data set, especially the removal of the liverwort outgroups and species of bryopsid mosses, permitted more of the data to be included in analyses because alignment of more variable regions could be accomplished without unacceptable ambiguity. In addition, sequences from three additional loci were added to the concatenated data: *nad5* from the mitochondrial genome and *rpoC1* and *psbT* from the plastid genome.

The 60-taxon, 8-locus data set was used in a companion paper (Shaw et al., 2010) to the present one, describing the timeframe of diversification in Sphagnopsida, and GenBank accession numbers were reported in that paper. For the sake of completeness, all GenBank numbers, including those previously published as well as those newly generated for this paper, are provided in Appendix 1. The two data matrices used for these analyses are available in TreeBase (<http://treebase.org>, accession number TB2:10581).

**Phylogenetic analyses: 60-taxon, eight-locus data set**—Single-locus data sets of SSU, LSU, *rbcL*, *rps4*, *psbA*, *trnG*, *trnL*, and *nad7* sequences were aligned using the software MUSCLE (vers. 3.7; Edgar, 2004) with default options. Alignments were adjusted by eye using the program SEA VIEW (vers. 4; Galtier et al., 1996); regions of ambiguous alignment were identified and excluded from further analysis. Taxa with identical sequences after exclusion of ambiguous regions were reduced to a single taxon representative before the analyses were conducted to reduce the computational effort required—the excluded taxa were later restored to the trees when represented graphically. Optimal substitution models were selected to maximize the Akaike information criterion (AIC) statistic for each locus using the software MrModeltest (vers. 2.3; Nylander, 2004) in conjunction with the program PAUP\* (vers. 4.0b10; Swofford, 1998).

Maximum likelihood (ML) bootstrap analyses were conducted (300 replicates) on each individual gene using the program RAxML (vers. 7.0.4; Stamatakis, 2006; Stamatakis, et al., 2008). All genes were analyzed using the optimal models, except *trnL* whose optimal model Hasagawa-Kishino-Yano (HKY) is not implemented in RAxML. For *trnL*, the best model identified by AIC and implemented in RAxML was used; i.e., the general time-reversible model (GTR).

Each gene data set was analyzed with the Bayesian Markov chain Monte Carlo (MCMC) inference software p4 (Foster, 2004) using the optimal model

plus a polytomy prior (resolution class prior with  $C = \log_e(10)$ ; Lewis et al., 2005), and with a single composition vector (i.e., the composition was tree-homogeneous). The composition homogeneity of each data set was tested using simulations of the posterior predictive distribution (PPD) (Bollback, 2002) of the  $\chi^2$  statistic (Foster, 2004). If the data were shown to fail the PPD test of homogeneity, successive additional composition vectors were added using the node discrete composition heterogeneity model (NDCH; Foster, 2004; Cox et al., 2008) until the model composition fit the data (i.e., the  $\chi^2$  statistic of the data could no longer be rejected as falling outside the simulated distribution at a  $P < 0.05$  level of significance). The multiple composition tree-heterogeneous NDCH models were considered optimal when the model composition fit could not be rejected. Each MCMC analysis was run for 2 000 000 generations with four parallel chains (i.e., Metropolis-coupled MCMC), and free parameter tuning values were automatically determined prior to the start of the MCMC. “Mixing” of the MCMC chains and effective sample size (ESS) scores of parameters were monitored so that the correct behavior of the MCMC could be assessed. Symmetrical mixing among adjacent chains and ESS values in excess of 300 were considered indications that the chain was behaving well. If the mixing was found to be inadequate the MCMC temperature parameter was adjusted and the chain restarted. If the ESS values were too low the chain was run for additional generations.

For all the MCMC described here, the “burnin” of each MCMC was determined by visual inspection of the log likelihood score across the sampled generations. Log marginal likelihoods of all MCMC analyses were calculated using eq. 5 of Newton and Raftery (1994) as implemented in p4.

A combined data set of the 60 taxa for the eight individual loci was constructed with previously identified ambiguous regions removed. All taxa had unique sequences across the combined eight genes. The optimal single model for the combined data set was determined by MrModeltest as described above. ML bootstrap analyses were conducted with 300 replicates using RAxML with a data-homogeneous (GTR+ $\Gamma$ ) model. In addition, a data-heterogeneous ML bootstrap analysis (300 replicates) was conducted using a separate model (GTR+ $\Gamma$ ×8) for each gene partition. Homogeneous MCMC analyses were conducted using MrBayes (vers. 3.1.2; Ronquist and Huelsenbeck, 2003) under a GTR+I+ $\Gamma$  model for 2 000 000 generations with the default two runs (each of four chains). Convergence between the two chains was assumed when the average standard deviation of split frequencies fell below 0.0001. Similar tree- and data-homogeneous MCMC analyses, but including a polytomy prior (GTR+I+ $\Gamma$ +P, other settings as above), were run in p4 for 2 000 000 generations as described previously. Model data-homogeneous but composition tree-heterogeneous (NDCH) analyses with two composition vectors and the polytomy prior (GTR+I+ $\Gamma$ +NDCH(2)+P) were conducted in p4 as described previously. A model data-heterogeneous and composition tree-heterogeneous MCMC analysis was conducted in p4 with a separate NDCH model for each partition (the optimal models found previously) with the polytomy prior and a partition-rate prior ([*ssu*:GTR+I+ $\Gamma$ +NDCH(2) + *lsu*:GTR+I+ $\Gamma$ +NDCH(3) + *rbcL*:GTR+I+ $\Gamma$ +NDCH(2) + *rps4*:GTR+ $\Gamma$ +NDCH(2) + *psbA*:GTR+I+ $\Gamma$ +NDCH(2) + *trnG*:GTR+ $\Gamma$  + *trnL*:HKY+ $\Gamma$  + *nad7*:GTR+ $\Gamma$ +NDCH(2)]+P+R).

Bayesian MCMC analyses were also conducted with the software Phylobayes (vers. 2.3c; Lartillot and Philippe, 2004) under the CAT model with a mixture of multiple GTR substitution models and a gamma distribution of rates among sites (CAT+GTR+ $\Gamma$ ). Two separate runs were conducted for ~1 380 000 cycles, and results compared between chains using the “bpcomp” program to ensure that the chains had converged. After discarding the burnin of each chain, tree and parameter estimates were determined by combining the results of both chains. Posterior predictive simulations of the  $\chi^2$  statistic were calculated using the Phylobayes software “ppred.”

**Phylogenetic analyses: Nine-taxon, 11-locus data set**—A nine-taxon combined data set was constructed with the previous eight genes plus *rpoC1*, *psbT*, and *nad5*. ML bootstrap analyses were conducted using RAxML with 300 replicates under the optimal model. Tree-homogeneous MCMC analyses were conducted in p4 using the polytomy prior, and tree-homogeneous NDCH analyses were conducted with the addition of a second composition vector. Phylobayes analyses under the CAT+GTR+ $\Gamma$  model were conducted for ~1 300 000 cycles in a single run. Further details of the analyses are as described previously for the 60-taxon data set.

**Genome size estimates**—*Sphagnum* is relatively conservative in chromosome number; only gametophytic numbers of  $N = 19$  and  $N = 38$  have been documented (Fritsch, 1982) although indirect evidence (genetic data and flow cytometric analyses) have identified two southern hemisphere species that appear to have triploid gametophytes (Karlin et al., 2009). Genome size estimates for *Ambuchanania*

*leucobryoides*, *S. inretortum*, and *S. sericeum* were undertaken to compare inferred ploidal levels in these species to gametophytically haploid and diploid taxa.

Flow cytometry (FCM) of herbarium samples was conducted using the Otto buffer system for isolating nuclei by chopping, propidium iodide as the DNA stain, and fresh *Solanum pseudocapsicum* (1C = 1.295 pg or 1266.5 Mbp; Tensch et al., 2010) as a pseudo-internal standard. A Partec CyFlow flow cytometer equipped with a green laser was employed as described in Ricca et al. (2008).

Determination of nuclear Feulgen DNA content (FDM) from herbarium specimens with DNA image analysis used methods described previously for fixed fresh material and herbarium specimens of *Sphagnum* (Ricca et al., 2008). Apical meristems were detached from herbarium specimens under distilled water so that the smallest embryonic leaves and the meristem itself were immediately exposed to fixative chemicals. Fixation time in 4% phosphate-buffered formaldehyde (pH 7) was 90 min at 20°C. In some instances (*Ambuchanania* [Buchanan 16981], *S. inretortum* [Price et al., 1236]), meristems were directly brought to 5N HCl without fixation. As a reference for staining intensity, embryonic meristems from dry seeds of *Pisum sativum* 'Kleine Rheinländerin' (2C = 8.84 pg; Greilhuber and Ebert, 1994) were processed synchronously and cut into pieces after about 5 min when softening had occurred. Formaldehyde was carefully removed with several rinses of methanol-acetic acid (3:1) for about 30 min. This postfixative was removed with several rinses of distilled water. Hydrolysis in 5 N HCl at 20°C was for 90 min (formaldehyde fixation) or for 60 min (no fixation), followed by a thorough wash in distilled water for 10 min. Staining in Schiff's reagent (Merck, Whitehouse Station, New Jersey, USA) was done for 90 min at 20°C. Schiff's reagent was washed out for 30 min with SO<sub>2</sub>-water. The material was briefly softened in 45% acetic acid and squashed onto glass slides, standard and unknown side by side. Coverslips were removed over a cold-plate after freezing. The slides were air-dried and kept light-protected until measurement, which occurred within 48 h.

Dye content of the Feulgen-stained nuclei was measured using the CIRES (Cell Imaging and Retrieval System, Kontron, Munich), with a Zeiss 63× oil Plan Neofluar objective, using Köhler illumination and the green channel of the video camera, a green interference filter, a neutral density filter, the shading correction option, and local background determination (around each measured nucleus separately). Almost all geometrically suitable moss nuclei of a slide were measured (114 on average, from 7–314 per slide; i.e., those automatically segmentable and in clear background) and a similar number of standard 2C nuclei, but mostly not more than 100, which is sufficient for a stable mean value.

DNA contents in Mbp (1C), were calculated using the ratio of moss nuclei (1C and 2C) vs. standard 2C nuclei corrected to 1C according to the replication state, multiplied by 8.84 pg or 8645.52 Mbp (conversion factor pg to Mbp = 978; Doležel et al., 2003).

## RESULTS

**Phylogenetic reconstructions: 60-taxon, eight-locus data set**—Total numbers of amplified nucleotides, numbers of nucleotides included in analyses after pruning regions of ambiguous

alignment, and optimal substitution models for each locus are provided in Table 1. Single-locus reconstructions under maximum likelihood and Bayesian inference are shown in Appendix S1 (see the Supplemental Data at <http://www.amjbot.org/cgi/content/full/ajb.1000055/DC1>, Figs. S.1.1–S.1.8 and S.1.9–S.1.16, respectively). The position of *Polytrichadelphus purpureus* with the outgroups in the *rbcL* NDCH analysis (Fig. S.1.11) appears to be anomalous and does not appear in the ML analysis of the data (Fig. S.1.3). No other significant incongruence was detected among single-locus reconstructions, and the eight loci were combined as a single concatenated matrix. A total of 4230 sites were excluded because of ambiguous alignment across the eight loci (Table 1). The combined matrix included 8498 nucleotide sites that were included in subsequent analyses. Of the 8498 included sites, 3380 represent the nuclear genome (nrDNA), 3378 the plastid genome, and 1740 the mitochondrial genome.

Phylogenetic reconstructions based on the combined eight-locus matrix were obtained using seven different combinations of analytical method (ML and Bayesian) and models of evolution (Table 2). The models ranged from a relatively simple homogeneous substitution pattern across taxa and sites, to one (model 6 in Table 2) with 123 parameters such that the analysis is both data heterogeneous for the substitution model and tree heterogeneous across each locus/partition. The Phylobayes CAT analysis (model 7 in Table 2) dynamically models composition heterogeneity across the data, but without having to prespecify which sites evolve under which composition (as in model 6).

Results of all analyses of the concatenated data are provided in online Appendix S1, supplemental Figs. S17–S25. Figure 1 shows the reconstruction from analyses under model 6 (Table 2), with bootstrap proportions and Bayesian posterior probabilities for critical nodes provided from that analysis and from three other models (see legend for Fig. 1). We focus here on relationships of *Ambuchanania* to other species traditionally classified in *Sphagnum*. Support for most other nodes on the tree are not shown; results from analyses of relationships within the class Bryopsida based on almost the same set of taxa and loci were described by Cox et al. (2004).

All analyses support the following inferences. The Sphagnopsida, including *Ambuchanania* and all species of *Sphagnum*, comprise a monophyletic group. Support is maximal under both ML and with all Bayesian models. A large group of *Sphagnum* species representing the traditional groups (subgenera or sections)

TABLE 1. Bayesian analyses of individual gene partitions for the 60-taxon, eight-gene data set.

Locus	Taxa	Incl. taxa <sup>a</sup>	Total sites	Incl. sites <sup>b</sup>	Optimal model <sup>c</sup>	P-value <sup>d</sup>	–log <sub>e</sub> (L <sub>m</sub> ) <sup>e</sup>
SSU	56	43	1896	1619	GTR+I+Γ+NDCH(2)+P	0.5784	4208.4413
LSU	60	50	2275	1761	GTR+I+Γ+NDCH(3)+P	0.0000 <sup>f</sup>	5987.1519
<i>rbcL</i>	59	55	1659	1282	GTR+I+Γ+NDCH(2)+P	0.9987	10187.1225
<i>rps4</i>	60	56	1063	568	GTR+Γ+NDCH(2)+P	0.6072	6094.2647
<i>psba</i>	59	52	1712	1144	GTR+I+Γ+NDCH(2)+P	0.7603	6766.5207
<i>trnG</i>	58	44	1089	204	GTR+Γ+P	0.0619	1811.1586
<i>trnL</i>	57	44	1055	180	HKY+Γ+P	0.4000	1183.5210
<i>nad7</i>	50	50	1979	1740	GTR+Γ+NDCH(2)+P	0.1881	5885.1619

<sup>a</sup> Number of taxa included in analyses after identical sequences were reduced to a single representative.

<sup>b</sup> Number of sites included after ambiguously aligned regions were excluded.

<sup>c</sup> Optimal model for each locus: the substitution rate matrices and among-site rate variation parameters were determined by MrModeltest, and the optimal number of composition vectors determined by posterior predictive simulations of the  $\chi^2_m$  statistic; +P indicates with the addition of the polytomy prior.

<sup>d</sup> P-value of the NDCH posterior predictive simulations of the  $\chi^2_m$  statistic.

<sup>e</sup> Log marginal likelihoods calculated according to the Eq. 16 of Newton and Raftery (1994).

<sup>f</sup> For the LSU data, three composition vectors did not fit:  $\chi^2_m$  statistic of original data: 124.3, range of statistic in posterior predictive simulations: 5.26 to 116.79 (in homogeneous data the range was 3.68 to 29.82).

TABLE 2. Analyses of the concatenated 60-taxon, 8-locus data set, and posterior probability values for particular clades.

Method	Model	$-\log_e(L_m)$	P-value <sup>a</sup>	A. + S.i. <sup>b</sup>	A. + S.i. + S.s. <sup>c</sup>
ML	1. GTR+I+ $\Gamma$	—	—	0.38	0.28
ML	2. (GTR+I+ $\Gamma$ )*8	—	—	0.42	0.26
Bayesian	3. GTR+I+ $\Gamma$	43571.4932	0.0000	0.96	0.49
Bayesian	4. GTR+ $\Gamma$ +I+P <sup>d</sup>	43605.0018	0.0000	1.00	0.00
Bayesian	5. GTR+ $\Gamma$ +I+NDCH(2)+P	43298.0001	0.9993	1.00	0.00
Bayesian	6. data- and tree-heterogenous+P+R <sup>e</sup>	42363.0379	—	1.00	0.02
	SSU: GTR+I+ $\Gamma$ +NDCH(2)	—	0.1596	—	—
	LSU: GTR+I+ $\Gamma$ +NDCH(3)	—	0.0000	—	—
	<i>rbcL</i> : GTR+I+ $\Gamma$ +NDCH(2)	—	0.1160	—	—
	<i>rps4</i> : GTR+ $\Gamma$ +NDCH(2)	—	0.5318	—	—
	<i>psba</i> : GTR+I+ $\Gamma$ +NDCH(2)	—	0.7384	—	—
	<i>trnG</i> : GTR+ $\Gamma$	—	0.6814	—	—
	<i>trnL</i> : HKY+ $\Gamma$	—	0.2182	—	—
	<i>nad7</i> : GTR+ $\Gamma$ +NDCH(2)	—	0.2182	—	—
Bayesian	7. CAT-GTR+ $\Gamma$	31205.3830	0.0602	0.99	0.56

<sup>a</sup> P-value of the NDCH posterior predictive simulations of the  $\chi^2_m$  statistic.

<sup>b</sup> Bootstrap support or posterior probability for the clade *Ambuchanania* + *Flatbergium inretortum*.

<sup>c</sup> Bootstrap support or posterior probability for the clade *Ambuchanania* + *Flatbergium inretortum* + *Eosphagnum sericeum* 858 + *E. sericeum* 1239.

<sup>d</sup> Polytoomy resolution class prior: C = log10.

<sup>e</sup> R: partition rate parameter.

*Acutifolia*, *Cuspidata*, *Polyclada* (*S. wulfianum*), *Rigida*, *Sphagnum*, *Squarrosa*, and *Subsecunda*, form a monophyletic group, also with maximal support from all analyses (Fig. 1, *Sphagnum*). Branch lengths appear extremely short within this clade, at least compared to branches throughout the rest of the tree. Nevertheless, monophyly of the traditional sections is significantly supported in most analyses (not shown in Fig. 1 but evident in Figs. S17–S25). The branches appear virtually nonexistent in Fig. 1 simply because they are very short relative to other branches in the reconstruction.

Two other species traditionally considered members of the genus *Sphagnum* fall outside *Sphagnum* s.s. (Fig. 1). Two samples of the Southeast Asian species, *S. sericeum*, are identical across all 8498 nucleotides included in these analyses but are together resolved as a separate clade of Sphagnopsida. *Sphagnum inretortum* of western South America is also resolved outside *Sphagnum* s.s. and is in fact strongly supported as sister to *Ambuchanania leucobryoides* by all Bayesian analyses, though not by ML bootstrapping (Fig. 1, Table 2). Relationships between *S. sericeum*, the clade containing *Ambuchanania* plus *S. inretortum*, and *Sphagnum* s.s. are not resolved; although all analyses converge on the inference that *S. sericeum*, *S. inretortum*, and *Ambuchanania* are outside the main clade of *Sphagnum*, no analysis supports *S. sericeum*, *S. inretortum*, and *Ambuchanania* in a single clade sister to *Sphagnum* s.s. (Table 2). Branch lengths indicate that these three taxa outside the main *Sphagnum* clade are each highly distinct at the molecular level compared to any species within *Sphagnum* s.s., even those in different traditional sections.

**Phylogenetic reconstructions: nine-taxon 11-locus data set**—Primarily because of the unexpected result from analyses of the 60-taxon, eight-locus data set that *Ambuchanania leucobryoides* and *Sphagnum inretortum* were resolved as sister species, we developed a second data set with fewer taxa and more nucleotide characters. During the course of this study, a second (Chilean) sample of *S. inretortum* became available so we included it in these analyses. The final analyzed data set included 11 705 nucleotide sites (Table 3), with 739 informative characters under parsimony. Base compositions of the individual loci and the concatenated data set are provided in Table 4.

Reconstructions from analyses of the concatenated 11-locus data set were rooted with *Andreaea* and *Takakia*. All analyses support a monophyletic Sphagnopsida with maximal support. Moreover, all analyses resolve three clades of Sphagnopsida, one including the two samples of *S. sericeum*, another including the two exemplars of *Sphagnum* s.s. (represented by *S. palustre* [section *Sphagnum*] and *S. lescurii* [section *Subsecunda*]), and the third including *Ambuchanania* plus the two samples of *S. inretortum*. The clade including *Ambuchanania* plus *S. inretortum* is supported by Bayesian posterior probabilities of 1.0 in analyses employing a homogeneous substitution model, and in two analyses employing heterogeneous models of varying complexity (see legend for Fig. 2). Under maximum likelihood, this clade is moderately supported by bootstrapping (0.71; Fig. 2). The two samples of *S. inretortum* are identical across all 11 705 nucleotides, as are the two samples of *S. sericeum*. It is worthy of note that although monophyly of *Ambuchanania* plus *S. inretortum* is strongly supported by these analyses, branch lengths show that they are phylogenetically divergent compared to, for example, *S. palustre* and *S. lescurii*, representing two sections within the traditional genus *Sphagnum*.

In an additional test of the inference that *Ambuchanania* and *S. inretortum* are sister taxa, rather than *Ambuchanania* being sister to all remaining Sphagnopsida, we constrained the tree in a Bayesian MCMC (GTR+I+ $\Gamma$ +NDCH(2)+P) to force the monophyly of *Sphagnum*, including *S. sericeum* and *S. inretortum*. This constraint forces a topology in which *A. leucobryoides* is the sister group to the rest of the Sphagnopsida. The constraint analysis tree had a marginal likelihood of  $-25727.9892$  (Table 3, model 5; online Fig. S.1.28), compared to the same analysis without the constraint:  $-25708.5622$  (Table 3, model 3; online Fig. S.1.24). The difference of 19.427 likelihood units favors the unconstrained analyses that places *Ambuchanania* as sister to *S. inretortum*. A Bayes Factor ( $2 \log_e(M1|M2) = 2 \times 19.427$ ) of 38.854 strongly favors this interpretation.

**Genome size estimates and inferences about ploidy**—With Feulgen image densitometry, positively stained nuclei were obtained from one (*Buchanan 16981*) of two *Ambuchanania* vouchers and from all five *Sphagnum* vouchers (Table 5). One

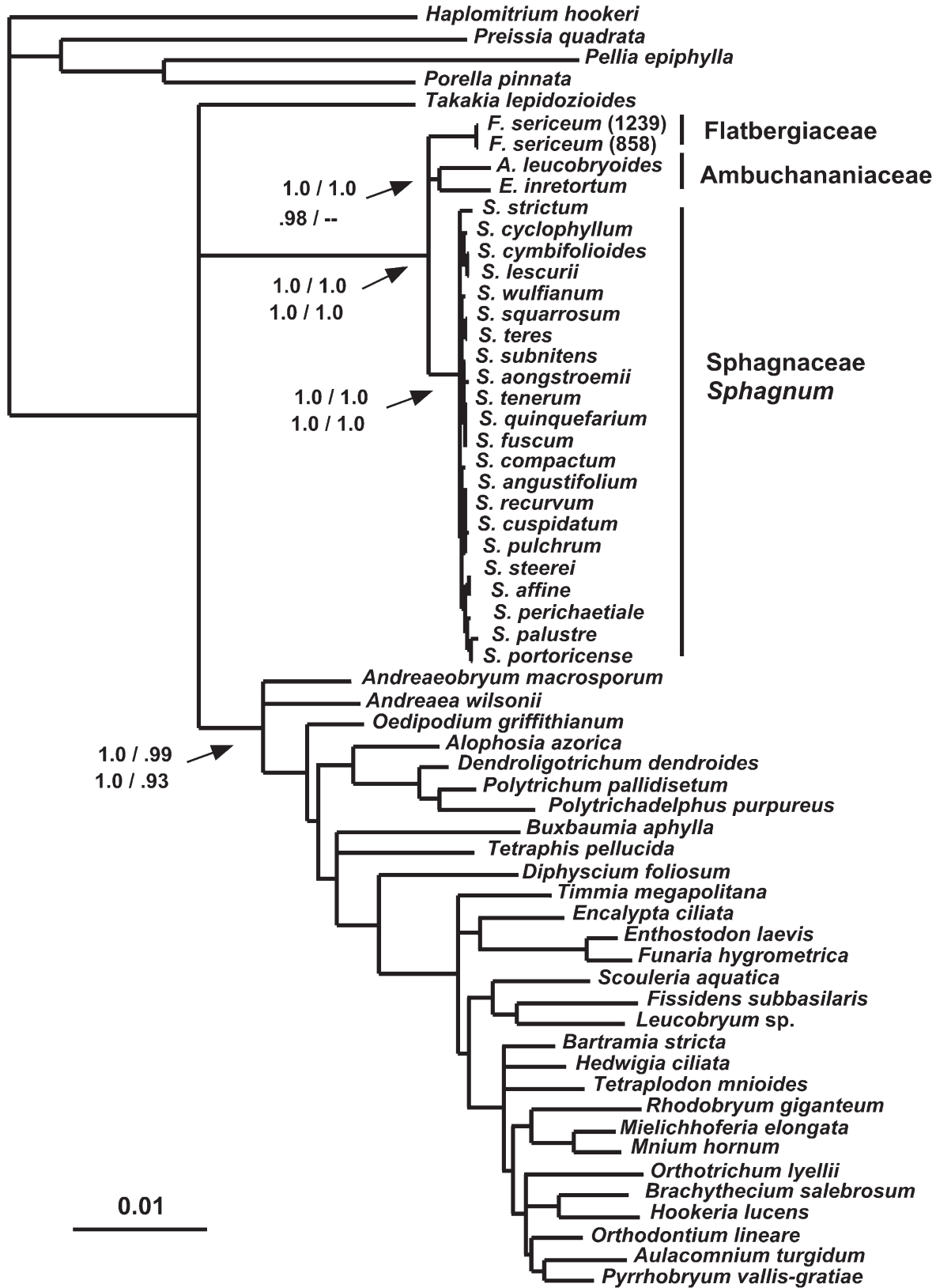


Fig. 1. Phylogram showing inferred relationships among mosses (Phylum Bryophyta) based on Bayesian analyses of the 60-taxon, eight-locus data set under the heterogeneous across-data across-tree substitution model (no. 6 in Table 2). Four support values associated with nodes are as follows (models listed in Table 2): upper left, model 5; upper right, model 6; lower left model 7; lower right, model 2.

TABLE 3. Analyses of the concatenated 9-taxon, 11-locus data set.

Method	Model	$-\log_e(L_m)$	$P^a$
ML	1. GTR+I+ $\Gamma$	—	—
Bayesian	2. GTR+ $\Gamma$ +I+P <sup>b</sup>	25813.5131	0.0000
Bayesian	3. GTR+I+ $\Gamma$ +NDCH(2)+P	25708.5622	0.3080
Bayesian	4. CAT-GTR+ $\Gamma$	21932.8669	0.0000
Bayesian	5. GTR+I+ $\Gamma$ +NDCH(2)+P+constraint <sup>c</sup>	25727.9892	0.4007

<sup>a</sup>  $P$ -value of the NDCH posterior predictive simulations of the  $\chi^2_m$  statistic.

<sup>b</sup> Polytomy resolution class prior:  $C = \log 10$ .

<sup>c</sup> A topological constraint was introduced so that *Ambuchanania* was the sister group to all “sphagnum” species.

recent *Ambuchanania* sample from 2008 had no embryonic leaves and exhibited no nuclei at all, perhaps because there was cytoplasmic decay before drying occurred. Flow cytometry was unsuccessful as well. Previous experience has shown that *Sphagnum* herbarium specimens (1) give progressively lower Feulgen readings with increasing age, and (2) require optimal drying for good results. It was thus expected that specimens as old as 29 yr would result in data that could only be regarded as minimum values for genome size, which in vivo would almost certainly be higher. Nevertheless, the size of the nuclei could be used as additional criterion for inferring ploidy. For comparison, a voucher of *S. girgensohnii* from 1990 was Feulgen-stained. Two slides from two capitula of this sample had 1C-values of 271.3 and 312.2 Mbp, indicating high interslide variation (here 1.15-fold) and 0.58 to 0.71-fold reduced staining compared to fresh material, for which 1C = 442–467 Mbp has been reported (Temsch et al., 1998; Bennett and Leitch, 2005).

Comparison of FDM with an FCM estimate was possible for the Chilean sample of *S. inretortum*, which was only 6 mo old and therefore recent enough that reliable genome size data could be obtained using both methods. This species had 353.7 Mbp (a relatively low haploid value) with FCM and maximally 292.8 Mbp with Feulgen densitometry, 0.83-fold lower than the FCM-derived value. This indicates some decay of DNA during preservation over the 6-mo period because fresh vouchers typically give similar values with FDM and FCM (Ricca et al., 2008). Five slides (branch tips) were measured with FDM and varied 1.14-fold between 256.3 and 292.8 Mbp. For *S. inretortum*, nine slides (branch tips) yielded values between 212.4 and 289.8 Mbp (1.36-fold variation). The lowest FDM values

TABLE 4. Bayesian analyses of individual gene partitions for the nine-taxon, 11-locus data set, listing the number of taxa included in each analysis, total nucleotide sites in each partition, numbers of included (Incl.) sites (after exclusion of sites because of ambiguous alignment), and numbers of parsimony informative (Pars. inf.) sites.

Locus	Taxa	Total sites	Incl. sites	Pars. inf.
SSU	9	1823	1775	64
LSU	8	2141	1957	40
<i>rbcl</i>	9	1455	1099	87
<i>rps4</i>	9	932	586	73
<i>rpoC1</i>	7	803	803	82
<i>psbA</i>	9	1719	1267	71
<i>psbT</i>	8	540	453	36
<i>trnG</i>	8	850	487	51
<i>trnL</i>	9	918	293	29
<i>nad5</i>	9	1938	1120	119
<i>nad7</i>	9	1935	1865	87

(Table 5) were, not surprisingly, recorded for *S. sericeum* collected in 1982 and 1980 (i.e., vouchers 26 and 28 yr old).

For *Ambuchanania*, a sample approximately 1 yr old yielded an estimate of 256 Mbp from one meristem, with a CV of 5.3% in 1C nuclei, which is normal. The nuclei appeared shrunken and irregular in form, but well stained. Their size was relatively small, and the nuclear DNA content implies a ploidal level of not more than haploidy, provided the genome is comparable in structure to a *Sphagnum* genome.

The high and certainly artifactual variation between slides of one sample made it futile to use mean values of accessions as a best-estimate of genome size. Rather, the slides with highest Feulgen values and therefore least DNA loss were considered the best estimates for inferring ploidal level (Table 5). In summary, genome sizes for all five *Sphagnum* samples and *Ambuchanania* are small enough to exclude the possibility that they correspond to polyploid species of *Sphagnum* (i.e., diploid gametophytes,  $N = 38$ ). One cannot, however, exclude the possibility that the particularly low values in *S. sericeum* indicate an even smaller genome size and chromosome number than is typical for haploid sphagna, which have 1C-values between 383 and 495 Mbp, while diploid species have between 796 and 931 Mbp (Temsch et al., 1998). This ranks relatively low but well within the bryophyta, with mosses (Voglmayr, 2000) having 1C-values between 170 and 2112 Mbp, and liverworts between 206 and 7791 Mbp (Temsch et al., 2010).

**Morphological observations**—We describe here the salient morphological characteristics of the three taxa resolved by phylogenetic analyses as outside the core clade of *Sphagnum* species, but within the deeper Sphagnopsida clade. Our focus is on those features that agree, or not, with typical morphological traits of species traditionally included in the genus *Sphagnum*. More exhaustive descriptions of morphology for *S. sericeum* was provided by Eddy (1977), for *S. inretortum* by Crum (1990, 2001a), and for *Ambuchanania leucobryoides* by Yamaguchi et al. (1990).

*Sphagnum sericeum*—In terms of whole-plant architecture, *S. sericeum* is a “mainstream” *Sphagnum*. Sporophytes are borne on pseudopodia as in other *Sphagnum* species; there are abundant pseudostomata among the capsule exothecial cells (Fig. 3A). Aside from an unusually glossy appearance of the gametophytes (when dry), the plants do not stand out as aberrant relative to other species of *Sphagnum*. They are relatively robust, to 10 cm or more in length, with well-developed terminal capitula and lateral branches in fascicles of 3–4 (Fig. 3A). Within each fascicle, there are typically two spreading branches and 1–2 pendent branches. In cross-section, the stems have a small central zone of thin-walled cells surrounded by a well-defined region of small thick-walled cells (the so-called wood-cylinder), as in most species of *Sphagnum*. On the outside, there is an abruptly differentiated cortex with (2–)3 layers of enlarged thin-walled cells (Fig. 3B). The cortex of branches consists of rectangular nonporose cells and well-differentiated retort cells (Fig. 3C).

The stem leaves of *S. sericeum* are ovate-triangular with abruptly acute to cuspidate apices (Fig. 3I). The branch leaves are more gradually acute to acuminate, widest at about midleaf (Fig. 3J). Perichaetial leaves are larger than vegetative stem or branch leaves, with gradually acuminate apices (Fig. 3D).

It is the structure of the leaf cells that sets *S. sericeum* apart from most other species of *Sphagnum*. Most significantly,

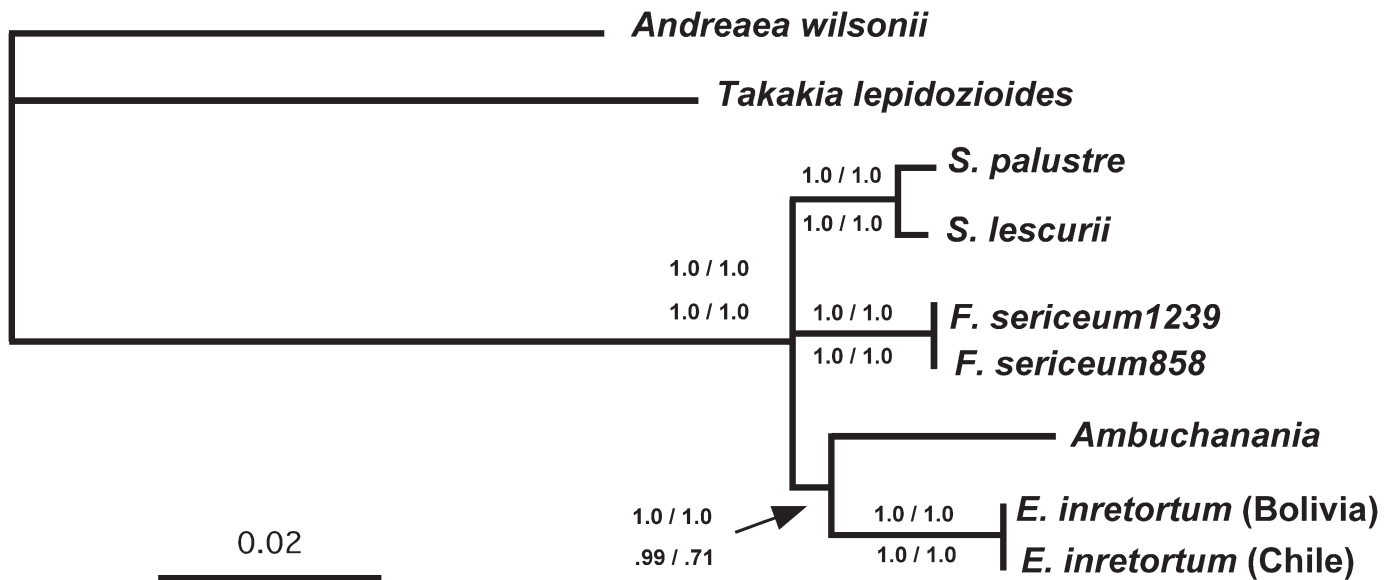


Fig. 2. Phylogram showing inferred relationships among *Sphagnum lescurii*, *S. palustre*, *Flatbergium sericeum*, *Eosphagnum inretortum*, and *Ambuchanania leucobryoides*, rooted with *Andreaea (Acroschisma) wilsonii* and *Takakia lepidozoioides* based on Bayesian analyses of the nine-taxon, 11-locus data set under the heterogeneous plus polytomy prior model. Four support values associated with nodes are as follows: upper left, heterogeneous plus polytomy; upper right, homogeneous plus polytomy, lower left, data heterogeneous CAT; lower right, homogeneous ML.

*S. sericeum* is one of only about three species of *Sphagnum* that lack fibrils on the walls of the hyaline leaf cells (Figs. 3G, H, K). Each cell typically has a single pore near the distal end on the outer (convex) surface. Compared with most other species of *Sphagnum*, there is a more irregular pattern of chlorophyllose and hyaline cells in *S. sericeum*, with patches of hyaline cells (Fig. 3G) rather than the more typical and very regular arrangement of one broad hyaline cell surrounded by four narrower chlorophyllose cells. Patches of cells such as observed in *S. sericeum* (and occasionally in other sphagna) likely reflect either transformation of chlorophyllose into hyaline cells during development, or additional symmetric cell divisions during leaf ontogeny (Butterfass, 1992). Leaf cells along the leaf margins sometimes protrude as serrulations (Fig. 3L), a feature common throughout the bryopsid mosses, but otherwise unknown in *Sphagnum*.

*Sphagnum inretortum*—This is a robust plant, pale whitish-green and somewhat reminiscent of species in *Sphagnum* section *Sphagnum* (Fig. 4A, B). When Crum (1990) described

*S. inretortum* from Bolivia he proposed a new section of *Sphagnum* to accommodate it (sect. *Inretorta* H. A. Crum). The main feature, as the name suggests, was the absence of retort cells in the branch cortex. Crum noted that the branch leaves of *S. inretortum* have a marginal resorption furrow (as in sections *Sphagnum*, *Rigida*, and a few species of *Acutifolia*) but lacks the cucullate branch leaf apices and fibrillose stem and branch cortical cells of section *Sphagnum*. He compared *S. inretortum* to species in sections *Rigida* and *Subsecunda* (the latter because of similarities in stem cross sectional anatomy) but eliminated these sections from consideration because of various incompatibilities. About 10 years later, Crum (2001a) described *S. lapazense*, also based on plants collected in Bolivia. The type collection of *S. lapazense* was collected in Departamento La Paz, as was *S. inretortum*, and the plants are very similar. Crum (2001a), however, assigned *S. lapazense* to the section *Sphagnum*. An additional collection that is very similar morphologically to the types of *S. inretortum* and *S. lapazense* was recently collected in Chile (J. Larraín and R. Andrus, unpublished data). Although there are some seemingly significant anatomical

TABLE 5. Nuclear Feulgen DNA contents for herbarium specimens of *Ambuchanania* and *Sphagnum* species. Values for 1C nuclei from slides with worst (lowest) and best (highest) staining are shown. If not indicated otherwise, samples were processed using formaldehyde fixation

Species	Collector, voucher	Year (age, yr)	Feulgen DNA content, 1C Mbp (N; CV%)		
			No. of slides	Lowest slide	Highest slide
<i>Ambuchanania</i>	Buchanan, 16981	?	1	—	256.0 (150; 5.78) <sup>a</sup>
<i>S. sericeum</i>	Damman & Larsen, A81386	1982 (17)	2	128.5 (30; 6.45)	185.6 (100; 4.65)
<i>S. sericeum</i>	Lai, 11370	1980 (29)	1	—	127.7 (223; 10)
<i>S. sericeum</i>	Yamaguchi et al., 18926	2000 (9)	1	—	223.1 (54; 9.62)
<i>S. inretortum</i>	Price et al., 1236	1999 (10)	9	212.4 (100; 3.92)	289.8 (34; 5.88) <sup>a</sup>
<i>S. inretortum</i> <sup>b</sup>	Andrus, 11835	2008 (<1)	5	256.3 (49; 8.62)	292.8 (100; 4.48) <sup>b</sup>
<i>S. girgensohnii</i>	R. Krisai <sup>c</sup>	1990 (19)	2	271.3 (251; 7.35)	312.2 (251; 5.13)

<sup>a</sup> HCl hydrolysis occurred without previous fixation.

<sup>b</sup> 1C = 353.7 Mbp estimated using flow cytometry.

<sup>c</sup> Lungau, Salzburg, Lessachtal, "Bacherlalm," 1 July 1990.



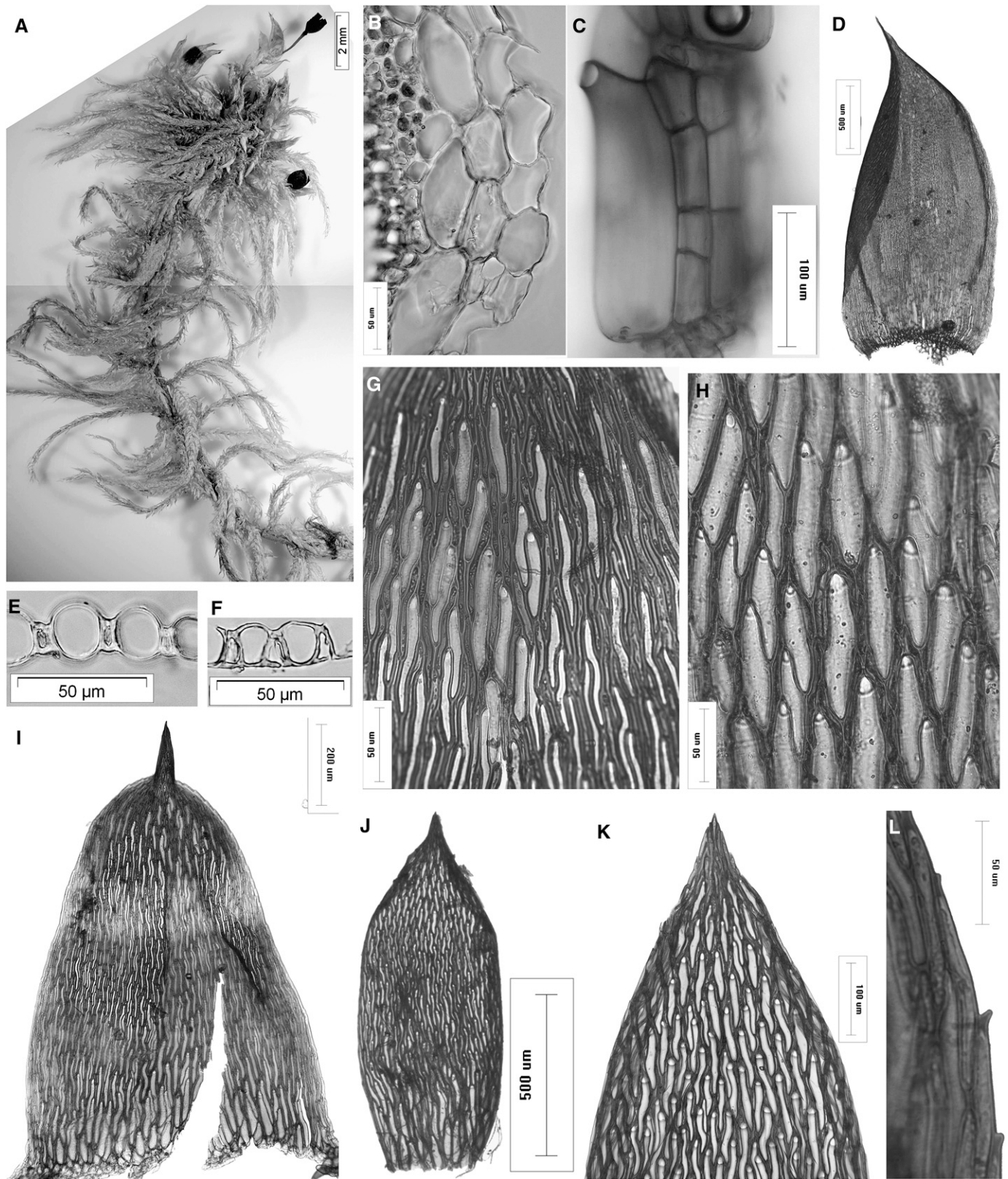


Fig. 3. Morphological characters of *Flatbergium sericeum*. (A) Gametophyte plant bearing sporophytes (Carr 15198). (B) Stem, transverse section (Yamaguchi 18295). (C) Branch cortex, showing retort cells and smaller nonporose cells (Carr 15198). (D) Perichaetial leaf (Yamaguchi 18295). (E, F) Branch leaf, transverse sections (Carr 15198). (G) Upper stem leaf cells, inside surface (Yamaguchi 18295). (H) Upper stem leaf cells, outside surface (Carr 15198). (I) Stem leaf (Yamaguchi 18295). (J) Branch leaf (Yamaguchi 18295). (K) Upper branch leaf, outside surface (Yamaguchi 18295). (L) Upper branch leaf, marginal cells (Carr 15198). All voucher specimens in DUKE.

differences between these three specimens (discussed below), we currently interpret them as conspecific and refer to them as *S. inretortum*. We were not able to obtain sequence data from the type of *S. inretortum*, but the type of *S. lapazense* and the recent Chilean collection are identical across 11 705 nucleotide characters. The species-level systematics of *S. inretortum* is worthy of additional study when additional collections come to light.

In cross section, the stems in all three collections have a central zone of thin-walled cells internal to a gradually differentiated wood cylinder of thicker-walled cells and a single layer of thin-walled cortical cells (Fig. 4E). Species of section *Sphagnum* are characterized by a multistratose cortex, typically with three layers of enlarged thin-walled cells. Stem leaves of the Chilean specimen are ovate and broadly acute, broadest about midway up the leaf (Fig. 4G). Stem leaves of the *S. inretortum* and *S. lapazense* type specimens have straighter margins and somewhat more abruptly narrowed apices, but it was difficult to isolate well-formed stem leaves from either specimen. A stem leaf from the *S. inretortum* specimen (Fig. 4H) is lingulate-oblong and broadly acute and that of the *S. lapazense* specimen is similar (not shown).

Branches in all three specimens (the types of *S. inretortum* and *S. lapazense*, and the Chilean collection) lack cortical retort cells. Rather, all cortical cells are elongate-rectangular and apopore (Fig. 4C). Branch leaves in the three specimens are similar in shape, but those of the Chilean specimen are substantially larger (Fig. 4I–K). The branch leaves have weakly inrolled apices, not as cucullate as is characteristic of species in section *Sphagnum*, though more so than is typical of plants in other sections. They lack the resorption of outer hyaline cell walls near the leaf apices; such resorption is highly characteristic of species in section *Sphagnum*.

Branch leaves have stout, sometimes branched fibrils (Fig. 5E–I). On the outer surface, the hyaline cells have irregular longitudinal pleats that seem to derive from some kind of cuticular layer (Fig. 5G–I, best seen in the type of *S. lapazense*; Fig. 5G). This feature appears to be associated with the fact that plants are exceptionally difficult to wet because they very slowly take up even hot water.

Stem leaf cells of the Chilean plants (Fig. 5C) have abundant, round outer pores and few inner pores, whereas the *S. lapazense* (Fig. 5D) and *S. inretortum* (not shown) types have few outer pores but abundant, round inner pores. Paralleling differences in pore patterns on the inner and outer hyaline cell surfaces of stem leaves among the three collections, branch leaves also differ in pore patterns on the inside and outside surfaces of the hyaline cells. The Chilean plants (Fig. 5I) and the type of *S. inretortum* (Fig. 5H) have abundant round pores on the outer surfaces of the hyaline cells but few scattered pores on the inner surfaces (*S. inretortum* shown in Fig. 5F). In contrast, the type of *S. lapazense* has few or no pores on the outer surfaces (Fig. 5G) and abundant, round pores on the inner surfaces (Fig. 5E).

All three specimens have branch leaf chlorophyllose cells that are lenticular and included, or nearly so, in transverse view (Fig. 4M, N). They all also have a marginal resorption furrow that can be seen either in transverse view (Fig. 4L) or as a ragged leaf margin in surface view (Fig. 5D).

Some of the Chilean plants had sporophytes borne on pseudopodia (Fig. 4A), as did some plants in the type of *S. inretortum* (Fig. 4D). The sporophyte exothecial cells are short-rectangular as is typical for *Sphagnum*, and pseudostomata are abundant (not shown). The pseudopodia in the Chilean plants are barely exerted from the bushy capitulum, whereas those in the *S. inre-*

*tortum* type are conspicuously elongate (Fig. 4D). Well-developed perichaetial leaves are carried upward on the pseudopodia of the *S. inretortum* type, and these are gradually differentiated in size and shape from the vegetative leaves (Fig. 4F). Upper cells of perichaetial leaves tend to be devoid of pores, and the fibrils consist of stout but incomplete thickenings (Fig. 5A, B).

Despite the presence of sporophytes in two of the three collections, we did not observe antheridia, either on the same plants with sporophytes or on separate plants.

*Ambuchanania*—Unlike the previous two species, *Ambuchanania* is highly divergent in gross morphology and anatomical detail from any species of *Sphagnum*. The plants are relatively small, generally about 0.5–3 cm in length (and maybe longer but mostly buried in sand when growing) and without terminal capitula or branch fascicles (Fig. 6A, B). In nature, the plants are mostly buried in their sandy substrates, except for apical portions of the gametophytes. The leaves are exceptionally large, especially considering the diminutive size of the whole plants, and are erect and loosely imbricate wet or dry. Although fasciculate branching is absent, the plants can have lateral branches, which appear to be of two more or less distinct types, either slender with very small leaves (Fig. 6B, left arrow) or more stout with much larger leaves (Fig. 6B, right arrow). The slender branches with small leaves eventually do produce larger leaves (observed but not illustrated). Stems consist of more or less uniform cells in transverse section (Fig. 6C); a clear wood cylinder of thick-walled cells is absent, as are abruptly differentiated cortical cells. Branch axes have uniform cortical cells, and retort cells are absent (Fig. 6D). In transverse view, the branches are like slender stems.

Leaves have dimorphic hyaline and chlorophyllose cells (Fig. 6E). Viewed from the inner or outer convex surface, the hyaline cells are rounded hexagonal to rhombic (Fig. 6K). In transverse section, large hyaline cells that reach the inner concave and outer convex surfaces alternate in a fairly regular fashion with smaller triangular hyaline cells that are transversely adjacent to small lenticular to tear-drop shaped chlorophyllose cells (Fig. 6I). Developmental studies of how the dimorphic hyaline and chlorophyllose cells differentiate are needed, but the transverse adjacency of the smaller triangular hyaline cells and the chlorophyllose cells suggests that each pair may be derived from a cell division during leaf ontogeny. Their transverse adjacency results in the leaf being bistratose between the larger hyaline cells that extend from the inner to outer leaf surface. This pattern is fairly regular, but irregularities in cell division patterns are also apparent. The arrangement of hyaline and chlorophyllose cells making up leaves of *Ambuchanania* suggest a very different developmental sequence relative to the well-documented ontogeny in *Sphagnum* leaves; cell structure in the leaves of *S. sericeum* and *S. inretortum*, in contrast, do not suggest any significant deviation from the “normal” *Sphagnum* mode of development.

Along the leaf margins, hyaline cells become narrow and elongate, forming a strongly but gradually differentiated border (Fig. 6I, arrow). Cell wall fibrils and pores are essentially lacking on leaves of main stems; very sparse and tiny pores occur occasionally near the leaf bases (Fig. 6J, arrows). The long, tubular leaves of the short branches (Fig. 6B, right arrow), however, have highly differentiated leaf cells, especially distally, with strong wall fibrils (Fig. 6H) and remarkably large, strongly ringed pores on the inner surfaces (Fig. 6F, G). No other member of the Sphagnopsida has such large or uniquely ringed pores. In the upper leaf parts these pores occur one per cell (Fig. 6G).

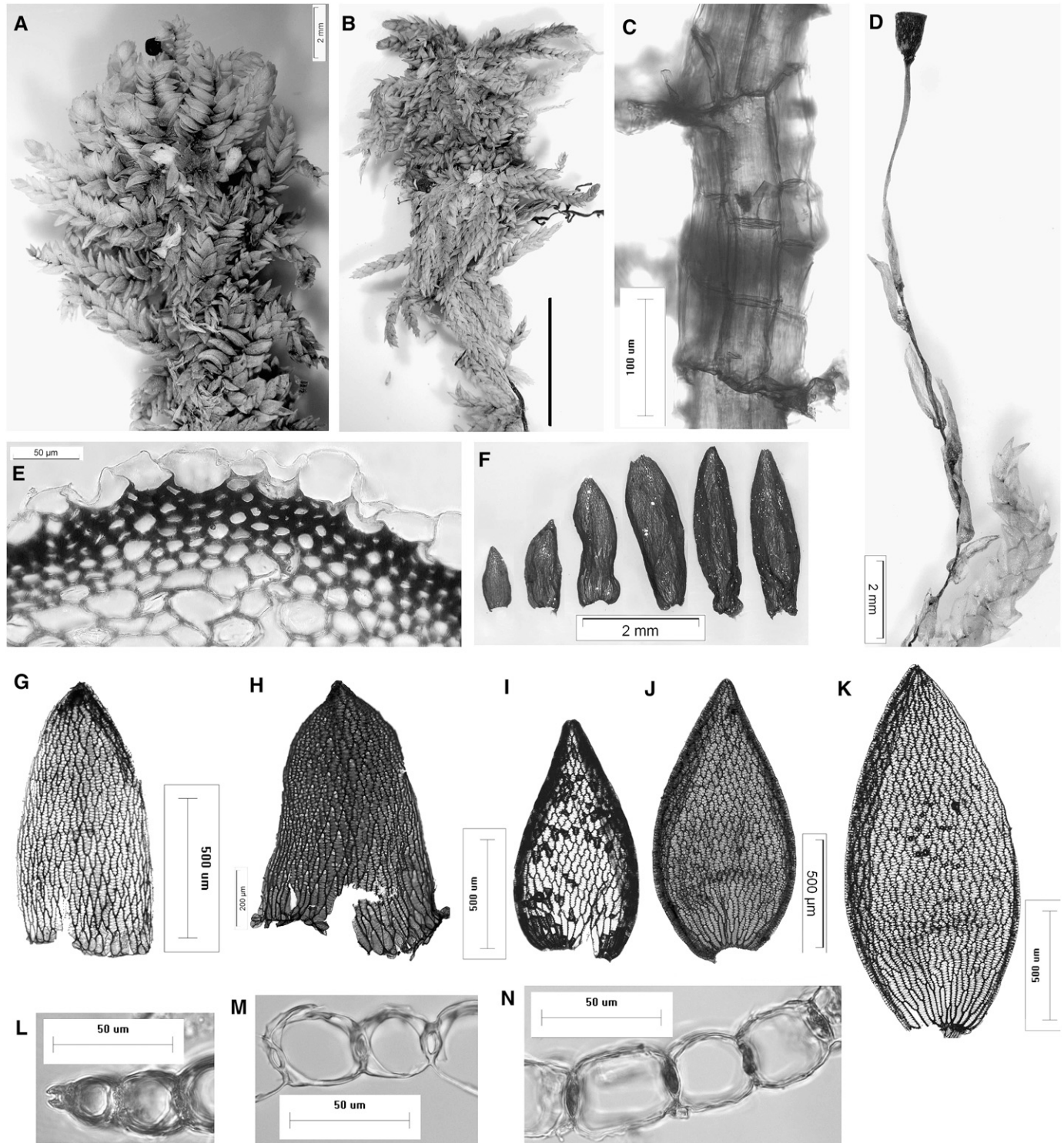


Fig. 4. Morphological characters of *Eosphagnum inretortum*. (A) Gametophyte plant bearing sporophytes (Larraín 31203). (B) Gametophyte plant (Feuerer, 1981). (C) Branch cortex showing absence of retort cells (Feuerer, 1981). (D) Pseudopodium with perichaetial leaves and terminal sporophyte (Feuerer, 1981). (E) Stem, transverse section (Feuerer, 1981). (F) Leaf transition from upper gametophyte to differentiated perichaetial leaves on pseudopodia (Feuerer, 1981). (G) Stem leaf (Andrus 11835). (H) Stem leaf (Feuerer, 1981). (I) Branch leaf (Price 1236). (J) Branch leaf (Feuerer, 1981). (K) Branch leaf (Andrus 11835). (L) Branch leaf marginal resorption furrow (Andrus 11835). (M) Branch leaf, transverse section (Andrus 11835). (N) Branch leaf, transverse section (Price 1236). All voucher specimens in DUKE.

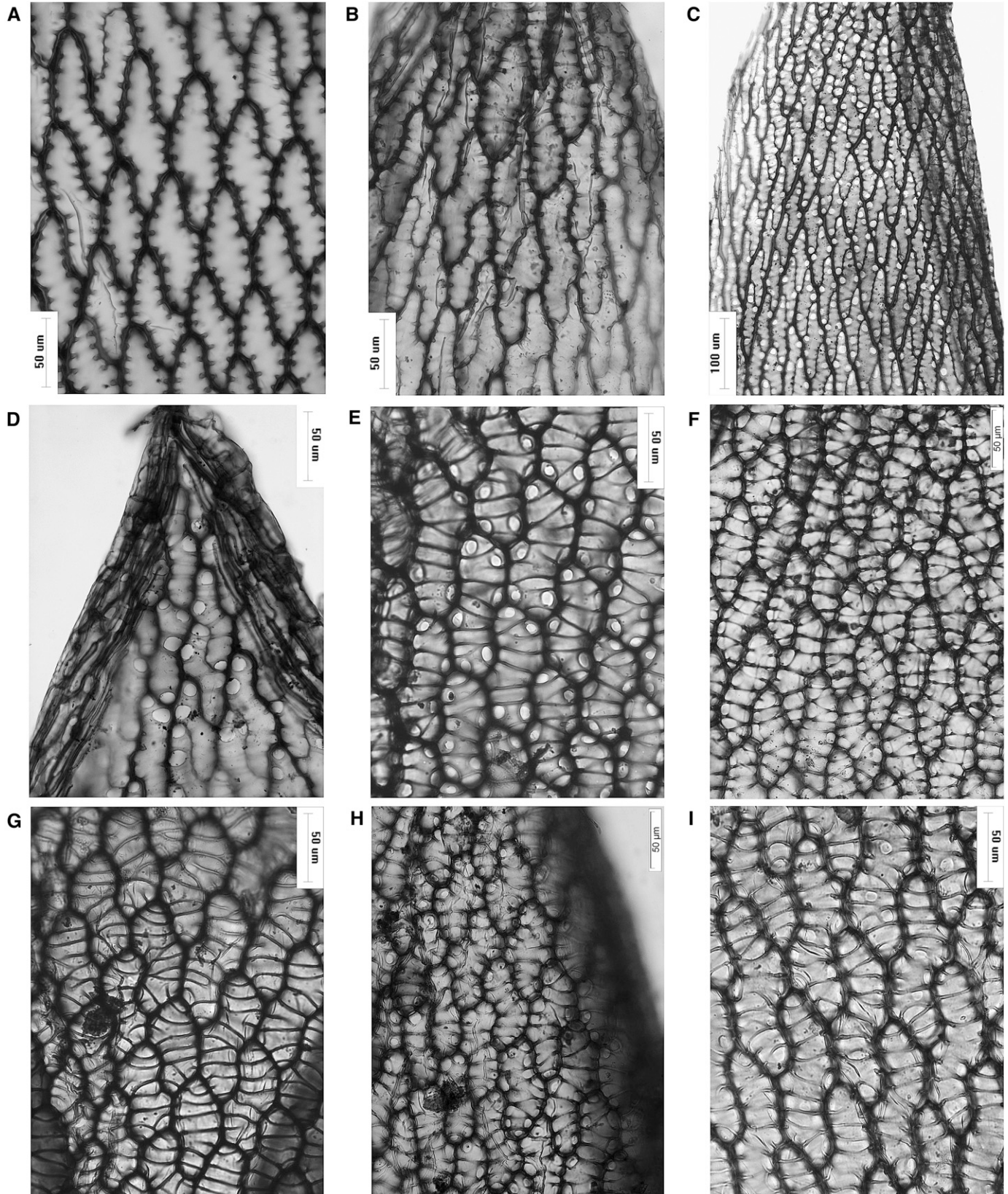


Fig. 5. Upper leaf cells of *Eosphagnum invetortum*. (A) Upper perichaetial leaf, outer surface (*Larrain 31203*). (B) Stem leaf, outer surface (*Price 1236*). (C) Stem leaf, outer surface (*Andrus 11835*). (D) Stem leaf, inner surface (*Price 1236*). (E) Branch leaf, inner surface (*Price 1236*). (F) Branch leaf, inner surface (*Feurerer, 1981*). (G) Branch leaf, outer surface (*Price 1236*). (H) Branch leaf, outer surface (*Feurerer, 1981*). (I) Branch leaf, outer surface (*Andrus 11835*). All voucher specimens in DUKE.

## DISCUSSION

**Proposed classification for the Sphagnopsida**—Faced with the problem of how to classify diversity within the Sphagnopsida in a way that best reflects phylogenetic relationships, the following observations are relevant. (1) There is a core clade of phylogenetically and morphologically cohesive group of species. (2) Species within that core clade are extremely closely related genetically/phylogenetically. (3) *Sphagnum sericeum* is unique morphologically relative to any species or groups of species within the core clade of *Sphagnum*. (4) *Ambuchanania leucobryoides* plus *Sphagnum inretortum* form a strongly supported clade that is also outside the core clade of *Sphagnum* species. (5) *Ambuchanania leucobryoides* and *S. inretortum* are highly divergent morphologically, and there are no apparent synapomorphies for the clade containing these two species.

We propose a new classification for the Sphagnopsida that takes each of these observations into account. *Sphagnum sericeum* is sufficiently distinct morphologically and, especially in terms of molecular divergence, to warrant recognition in a separate genus and family. Phylogenetic divergence relative to core *Sphagnum* species and the sister-group relationship between *Ambuchanania* and *S. inretortum* warrants the placement of these two taxa in a separate family, Ambuchananiaceae, in two separate genera. The remaining species, all closely related and traditionally classified in the genus *Sphagnum* are retained in that genus, classified as the Sphagnaceae. Segregation of *S. sericeum* and *S. inretortum* in families separate from *Sphagnum* (Sphagnaceae) will displease some, because both species have the capitulate gametophytes with fasciculate branching characteristic of that genus. However, this taxonomic solution best reflects phylogenetic relationships and evolutionary divergence. In terms of the practical consequences of this proposed taxonomic treatment of the Sphagnopsida, it is worth noting that all of the northern hemisphere work on peatland ecology will still deal exclusively with peatmosses classified in *Sphagnum*; the new classification will have little impact on this ecological field.

A primary division of *Sphagnum* into groups that correspond to subgenus or section *Sphagnum* vs. all other groups (Andrews, 1911) is not supported by molecular phylogenetic analyses (Shaw et al., 2003). *Sphagnum* is divided here into six subgenera corresponding to traditionally recognized groups (e.g., Lindberg, 1882; Warnstorf, 1911; Isoviita, 1966; Crum, 1984). The subgenus *Acutifolia* is divided into three sections to reflect close phylogenetic relationships between *S. wulfianum* (sect. *Polyclada*), *S. aongstroemii* (sect. *Insulosa*) and the core *Acutifolia* (sect. *Acutifolia*). Shaw et al. (2005) resolved a well-supported monophyletic group that includes the core *Acutifolia* plus *S. wulfianum* and *S. aongstroemii*. Within that clade, *S. wulfianum* and *S. aongstroemii* were resolved as the two earliest lineages paraphyletic to a monophyletic *Acutifolia* s.s. The current classification in which the subgenus *Acutifolia* includes all these taxa, with sections for *S. wulfianum* and *S. aongstroemii*, reflects the monophyly of the broader *Acutifolia* but also the morphological distinctions between sections *Polyclada*, *Insulosa*, and *Acutifolia*. Subgenus *Squarrosa* is sister to this inclusive subgenus *Acutifolia*.

**Order Sphagnales M. Fleisch.**, Die Musci der Flora von Buitenzorg 1: xxiii. 1904.

**Family Sphagnaceae Dumort.**, Analyze des Familles de Plantes 68. 1829.

**Genus Sphagnum L.**, Species Plantarum 1106. 1753. (type: *S. palustre* L.)

**Subgenus Sphagnum L.** (type: *S. palustre* L.)

**Subgenus Rigida (Lindb.) A. Eddy**, Bulletin of the British Museum (Natural History), Botany 5: 431. 1977.

**Subgenus Cuspidata Lindb.**, Musci Scandinavici 11. 1879.

**Subgenus Subsecunda (Lindb.) A. J. Shaw, comb. & stat nov.** Basionym: *Sphagnum* section *Subsecunda* Lindb., Öfversigt af Förhandlingar: Kongl. Svenska Vetenskaps-Akademien 19: 135. 1862.

**Subgenus Squarrosa (Russow) A. J. Shaw, comb. & stat nov.** Basionym: *Sphagnum* subsection *Squarrosa* Russow, Archiv für die Naturkunde Liv-, Ehst- und Kurlands, Serie 2, Biologische Naturkunde 7: 111, 140. 1865.

**Subgenus Acutifolia (Russow) A. J. Shaw, comb. & stat nov.** Basionym: *Sphagnum* subsection *Acutifolia* Russow, Archiv für die Naturkunde Liv-, Ehst- und Kurlands, Serie 2, Biologische Naturkunde 7: 111, 114. 1865.

**Section Acutifolia (Russow) Schimp.**, Synopsis Muscorum Europaeorum, Ed. 2, 825. 1876.

**Section Polyclada Warnst.**, Botanical Gazette 15: 225. 1890.

**Section Insulosa Isov.**, Annales Botanici Fennici 3: 231. 1966.

**Family Flatbergiaceae, A. J. Shaw, fam. nov.**

Plantae capituliis apicalibus, ramificatione fasciculata, foliis caulibus cuspidatis, cellulis folii e fibrillis poris singularibus. Type: *Flatbergium*.

**Genus Flatbergium A. J. Shaw, gen. nov.** Syn.: *Sphagnum* subgenus *Homophylla* Lindb., Öfversigt af Förhandlingar: Kongl. Svenska Vetenskaps-Akademien 19: 134. 1862. (Lectotype, designated here: *S. sericeum* Müll. Hal.), *non Homophyllum* Merino, Anales de la Sociedad Española de Historia Natural 1898: 108. 1898 (Blechnaceae); *Sphagnum* subsect. *Sericea* Warnst., *Sphagnum* sect. *Sericea* (Warnst.) M. Fleisch., nom. inval.

Latin diagnosis provided by Lindberg, Öfversigt af Förhandlingar: Kongl. Svenska Vetenskaps-Akademien 19: 134. 1862. With one species: *Flatbergium sericeum* (Müll. Hal.) A. J. Shaw, comb. nov. Basionym: *Sphagnum sericeum* Müll. Hal., Botanische Zeitung (Berlin) 5: 481, 484. 1847.

**Family Ambuchananiaceae Seppelt & H. A. Crum ex A. J. Shaw, fam. nov.**

Plantae heterogeneae in morphologia, synapomorphis molecularibus in DNA nuclei mitochondri et plasti unitae. Type: *Ambuchanania*.

**Genus Ambuchanania Seppelt & H. A. Crum ex A. J. Shaw, gen. nov.**

Latin diagnosis provided by H. A. Crum & R. D. Seppelt, Contributions from the University of Michigan Herbarium 22: 29. 1999. Type: *Ambuchanania leucobryoides* (T. Yamag., Seppelt & Z. Iwats.) Seppelt & H. A. Crum ex A. J. Shaw, comb. nov. Basionym: *Sphagnum leucobryoides* T. Yamag., Seppelt & Z. Iwats., Journal of Bryology 16: 45, f. 1–6. 1990.

With one species: *A. leucobryoides*.

**Genus Eosphagnum A. J. Shaw, gen. nov.**

Plantae capituliis et ramificatione fasciculata, caulibus cortice unistratosi, cortice caulium et ramorum e fibrillis, cellulis retortis destitutis, foliis sulco resorpto. Type: *Eosphagnum inretortum* (H. A. Crum) A. J. Shaw, comb. nov. Basionym: *Sphagnum inretortum* H. A. Crum, Bryologist 93: 283, f. 1–8. 1990. (Syn.: *Sphagnum lapazense* H. A. Crum, Contributions from the University of Michigan Herbarium 23: 107. f. 1: a–d. 2001.)

**Family Flatbergiaceae**—This family is described to accommodate *Flatbergium sericeum*. *Flatbergium sericeum* is currently known from a broad geographic range from New Guinea

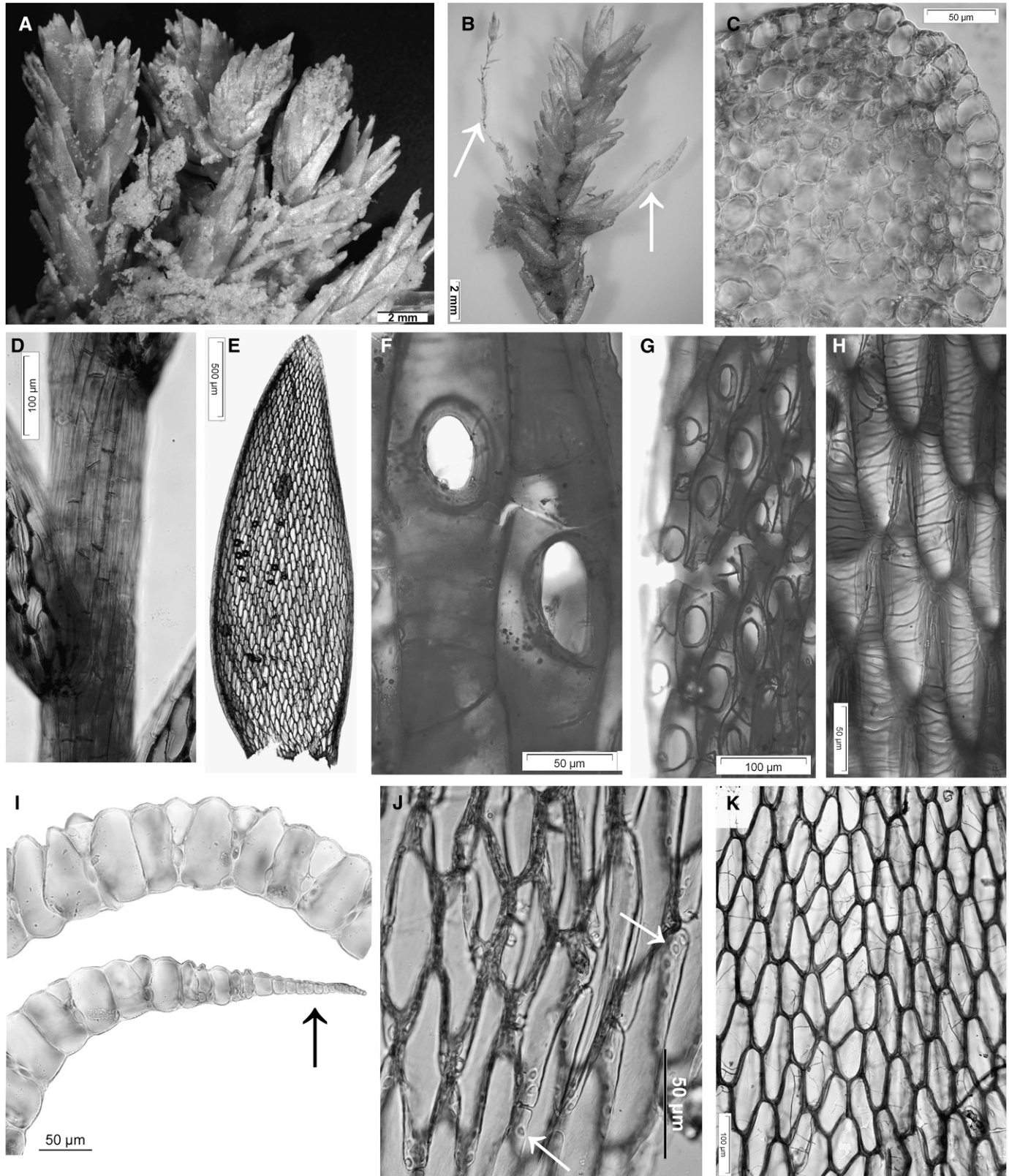


Fig. 6. Morphological characters of *Ambuchanania leucobryoides* (Buchanan 16981). (A) Gametophyte habit. (B) Gametophyte plant showing two branches (arrows): long branch (left) and short branch (right). (C) Stem, transverse section. (D) Branch cortex showing absence of retort cells. (E) Stem leaf. (F) Two leaf cell pores showing raised borders, upper part of leaf on short branch. (G) Leaf cell pores, upper part of leaf on short branch. (H) Upper cells of leaf from short branch showing fibrils. (I) Stem leaf transverse sections, median (above) and marginal (below); arrow indicates differentiated leaf border. (J) Base of stem leaf, inner surface, showing very small pores (arrows). (K) Upper stem leaf cells, outer surface. All voucher specimens in DUKE.

northward to China (Eddy, 1977; Li and He, 1999). Warnstorf (1911) classified *F. sericeum* in a group (at the subsectional level) that he called *Sericea*, along with the North American species, *S. macrophyllum* Brid. and *S. cribrosum* Lindb. [the latter as *S. floridanum* (Austin) Cardot]. He grouped these species together because they share the unusual feature of lacking wall fibrils in the branch and stem leaf hyaline cells. The only other species of *Sphagnum* that consistently lack leaf cell fibrils are *S. efibrillosum* A. L. Andrews and *S. novae-caledoniae* Paris & Warnst., both endemic to New Guinea. Eddy (1977) and Crum (1992) classified both *S. efibrillosum* and *S. novae-caledoniae* in the section *Subsecunda*, but considered *S. macrophyllum* and *S. cribrosum* as belonging to a different section, *Isocladus*. More recent phylogenetic evidence demonstrates (with strong support from multiple loci) that *S. macrophyllum* and *S. cribrosum* are also nested within section *Subsecunda* (Shaw et al., 2004); unfortunately, *S. efibrillosum* and *S. novae-caledoniae* have not been included in molecular phylogenetic analyses. The type specimen of *S. efibrillosum* (Papua New Guinea, *L. J. Brass 4473 NY!*) is morphologically quite similar to *S. macrophyllum* and is likely related within the section *Subsecunda*.

It is clear from the current results that *Flatbergium sericeum*, in contrast, is not a member of section *Subsecunda*, which is part of the core clade of *Sphagnum* (*Sphagnum* in Fig. 1). Morphologically, *F. sericeum* has distinctive features in addition to the absence of leaf cell wall fibrils, but none that would suggest a priori that the species is outside the core group of *Sphagnum* species. Eddy (1977) classified it in a monospecific subgenus *Homophylla* of *Sphagnum*, based on the lack of differentiation in size and shape between the stem and branch leaves, the absence of leaf cell fibrils, and the presence of single pores near the apices of leaf hyaline cells. None of these characters alone is absolutely unique within *Sphagnum*, but combined, they differentiate *F. sericeum* from any of the traditionally recognized sections. In transverse section, the shape of the branch leaf chlorophyllose cells, generally diagnostic for different sections of *Sphagnum*, are compatible with a placement for *F. sericeum* in the section *Subsecunda*. Eddy (1977) noted that the stem anatomy of *F. sericeum* is similar to species in the section *Cuspidata*. In his discussion of *F. sericeum* and the subgenus *Homophylla*, Eddy (1977) argued that the absence of leaf cell fibrils in *F. sericeum* is primitive, whereas their absence in *S. macrophyllum*, *S. cribrosum*, and *S. novae-caledoniae* represents secondary loss(es).

**Family Ambuchananiaceae**—When Crum and Seppelt (1999) segregated *Sphagnum leucobryoides* in its own genus, family, and order (*Ambuchanania*, *Ambuchananiaceae*, *Ambuchananiales*, respectively), they provided a single Latin diagnosis, which makes these names nomenclaturally invalid. Seppelt (2000) attempted to validate the *Ambuchananiaceae*, but because the genus name was still invalid, the family name also remained invalid. We here validate *Ambuchanania* (above). We choose not to separate the *Ambuchananiaceae* in a separate order distinct from the Sphagnales.

Both the 60-taxon, eight-locus data set and the nine-taxon, 11-locus data set provide strong support for a sister group relationship between *Ambuchanania* and *Eosphagnum inretortum*. Support for this relationship enjoys a 100% posterior probability under Bayesian inference regardless of the substitution model and mode of evolution (98% in one analysis). Maximum likelihood support is weaker; bootstrapping provided less than 50% support in the 60-taxon analyses, but 71% of the bootstrap replicates did resolve *E. inretortum* as sister to *Ambuchanania*

in the nine-taxon analysis. Despite lack of support for the sister-group relationship from bootstrapping in the ML analyses, *Ambuchanania* and *S. inretortum* were resolved as sister taxa in both optimal ML trees, as they were in all Bayesian reconstructions. The second data set was constructed in an attempt to refute the sister group hypothesis for *Ambuchanania* and *E. inretortum* after this relationship was resolved in the 60-taxon data set, but analyses with more genomic sampling provided even stronger support. When we constrained this tree to a topology with *Ambuchanania* sister to all other species of Sphagnopsida (including *F. sericeum* and *E. inretortum*), the constrained topology was significantly less likely than the unconstrained tree that resolved *Ambuchanania* and *E. inretortum* as sister taxa. We conclude that this relationship is accurate. For this reason, we classify *Ambuchanania* (with *A. leucobryoides*) and *Eosphagnum* (with *E. inretortum*) in the same family, *Ambuchananiaceae*.

**Genus *Eosphagnum***—*Eosphagnum inretortum* conforms to “mainstream” *Sphagnum* architecture at the whole-plant level, with terminal capitula, typical anatomy of stems and branches, fasciculate branching, and dimorphic leaf cells with the hyaline cells ornamented by pores and wall fibrils. The branch cortex lacks retort cells, but these are lacking in other *Sphagnum* species scattered across the genus. Differentiated retort cells are lacking in the sections *Sphagnum* and *Rigida* within the core clade of *Sphagnum*, although the cortical cells commonly have pores. In *S. macrophyllum* and *S. cribrosum* (section *Subsecunda*), the branches lack retort cells and cortical cells are aporose, very similar to those found in *E. inretortum*. Clearly, details of cortical cell morphology are labile within *Sphagnum*.

When he described *Sphagnum (Eosphagnum) inretortum* as a new species (as *S. lapazense*), Crum (2001a, p. 107) stated, “Because of the cucullate leaves with resorption furrows at the margins, the species clearly belongs in the section *Sphagnum*, although the leaves lack membrane gaps at the back of the apex and fibrils in the stem and branch cortex.” The elliptical shape of branch leaf chlorophyllose cells in transverse section is consistent with a placement in section *Sphagnum*, as are the large size and limited number of branch leaf pores.

Despite a superficial similarity to species of section *Sphagnum*, *Eosphagnum inretortum* has features inconsistent with that section. The stem cortex of section *Sphagnum* species is differentiated as 3–4 layers of enlarged hyaline cells, whereas the cortex in *E. inretortum* consists of a single layer of enlarged cells. Branch leaves of species in section *Sphagnum* are cucullate and have extensive resorption of cell walls on the outer convex surfaces near the leaf apices (the membrane pleats mentioned by Crum, 2001a); these features are both absent in *E. inretortum*. Crum (1990) cited this absence of resorption when he excluded *E. inretortum* from the section *Sphagnum*, but trivialized the difference when he chose to classify *S. lapazense* within the section *Sphagnum* 11 yr later (Crum, 2001a). Moreover, *E. inretortum* lacks fibrils in the stem and branch cortical cells, a feature characteristic of, though somewhat variable within, the section *Sphagnum*. Some species of the section do have the fibrils weakly developed, rudimentary, or virtually absent, but there is no hint of cortical cell fibrils in *E. inretortum*. The combination of morphological traits characterizing *E. inretortum* would seem to exclude the species from placement in any known section of *Sphagnum*. Some morphologically aberrant species (e.g., *S. macrophyllum*; *S. pylaiesii* Brid.) nevertheless appear to be phylogenetically nested within larger sections and the same could be true for *E. inretortum*. However, molecular data presented

in Shaw et al. (2003) and strongly corroborated here, demonstrate unambiguously that *E. inretortum* has no close relationship to the section *Sphagnum* or to the genus *Sphagnum*.

The species-level taxonomy of the genus *Eosphagnum*, which we currently consider to be monospecific, may need to be revisited in the future. We recognize a single species, *E. inretortum*, despite a level of variation in leaf pore structure that might in some cases distinguish different species in *Sphagnum*. Crum's (2001a) original protologue of *S. lapazense* was confused because his written description did not match his illustrations. In the text, he described the branch leaves in the type of *S. lapazense* as having few or no pores on the outer convex surfaces, with 4–9 round pores on the inner surfaces. This description agrees with our observations on the type collection (Price 1236). His illustrations, however, are reversed; his fig. 1b (Crum, 2001a) shows cells with round pores but is labeled as from the outer surface, and fig. 1c, labeled as the inner surface, shows cells with no pores. The latter shows the characteristic striations found on the outer surfaces of hyaline cells in all three collections of *E. inretortum* (illustrated in the current paper as Fig. 5G–I).

In contrast to the type of *Sphagnum lapazense*, the Chilean collection that we currently attribute to *Eosphagnum inretortum* has branch leaves with more conspicuous pores on the outer surfaces than on the inner surfaces (matching Crum's illustrations of *S. lapazense*, though not his description of that species)! In pore structure, the type of *E. inretortum* is intermediate between the Chilean collection and the type of *S. lapazense*, providing evidence that the differences among plants represent conspecific variation. Moreover, the Bolivian (*S. lapazense*) and Chilean samples were identical across the 11 705 nucleotides included in the nine-taxon, 11-locus data set. They do differ at one site in a variable part of the ITS (nrDNA) locus that was excluded from the formal analyses because it could not be aligned across all nine taxa.

**Genus *Ambuchanania***—When they first described *A. leucobryoides*, Yamaguchi et al. (1990) placed the species in a new section, *Buchanania*, of the genus *Sphagnum*. Crum and Seppelt (1999) reviewed the morphological features that set this species apart from other peat mosses and elevated the section to generic rank as *Ambuchanania* (because at the generic level the name *Buchanania* is preoccupied). Two genera have been segregated from *Sphagnum* over the years (i.e., *Isocladus* Lindb. for *S. macrophyllum*, *Hemitheca* (Lindb. ex Braithw.) Lindb., an invalid name proposed provisionally by Lindberg (1882) for *S. pylaesii*). However, neither of these segregate genera has been widely accepted.

*Ambuchanania leucobryoides* is far more distinct morphologically from any other species of *Sphagnum* than is *S. macrophyllum* or *S. pylaesii*. Unique morphological characteristics of *A. leucobryoides* were described in detail by Yamaguchi et al. (1990) and summarized by Crum and Seppelt (1999). The gametophytes are simple or sparsely and irregularly branched, a feature that is shared with some other species of *Sphagnum*, especially in the section *Subsecunda*. However, more significant than the difference in overall gametophyte architecture characterizing *Ambuchanania* are numerous unique anatomical features. The stem of *Ambuchanania* consists of more or less uniform cells with no differentiation of wood cylinder or enlarged cortical cells. Moreover, the leaves of *Ambuchanania* are partially bistratose and have a conspicuous border of linear cells, features with no counterparts in other *Sphagnum* species. The leaf cells are dimorphic, with chlorophyllose and hyaline cells,

but the arrangement of the two cell types is unlike that of any *Sphagnum* species, and although leaf development has not been documented in *Ambuchanania*, it is clear from the arrangement of hyaline and chlorophyllose cells that leaf ontogeny departs significantly from the regular pattern described for *Sphagnum* (Holcombe, 1984). Lateral branches in *Ambuchanania* are uncommon and are of two more or less distinct types: short and long branches (Yamaguchi et al., 1990). The leaves of these branch types differ in size, shape, and cellular anatomy. Pores and fibrils, both hallmarks of sphagnoid mosses, are better developed on the leaves of short branches.

As in *Sphagnum*, the sporophyte of *Ambuchanania* lacks a seta, and the capsule is instead raised on a pseudopodium of gametophytic origin. The sporophytes of *Ambuchanania* do not appear to differ in any significant way from those of *Sphagnum* and are presumed to share similar embryological features that distinguish *Sphagnum* from other mosses. The origin of sporogenous tissue from amphithecial rather than endothelial cells, as in other species of Sphagnopsida, is presumed to characterize *Ambuchanania*, although this needs to be confirmed. *Ambuchanania* has bisexual gametophytes and archegonia are borne in terminal clusters with the antheridia situated at the base of these clusters (Yamaguchi et al., 1990). *Sphagnum* can have uni- or bisexual gametophytes, and the perichaetia (archegonia and surrounding leaves), in contrast to *Ambuchanania*, are not terminal on the main stem but are rather on short branches near the stem apices. The antheridia are produced on catkin-like branches in the capitula well removed from the perichaetia in *Sphagnum* species with bisexual gametophytes. The antheridia of *Ambuchanania* are oblong-elliptical, similar to those of other mosses but unlike the globose antheridia of all *Sphagnum* species.

**Implications of *Sphagnopsida* phylogeny for morphological evolution**—Although the relative timing of phylogenetic branching among the three major clades of Sphagnopsida is unresolved, the sister-group relationship between *Eosphagnum* and *Ambuchanania* implies that the simple and highly divergent gametophyte morphology of *Ambuchanania* is derived rather than primitive. Regardless of whether *Flatbergium sericeum* diverged first and the *Ambuchanania* plus *Eosphagnum* clade is sister to the core *Sphagnum* clade, or *Ambuchanania* plus *Eosphagnum* diverged first, our phylogenetic results favor the interpretation that *Ambuchanania* evolved from an ancestor that had “mainstream” *Sphagnum* architecture, i.e., fasciculate branching, a terminal capitulum, and dimorphic leaf cells comprising unistratose leaves. Although both *Ambuchanania* and *E. inretortum* lack retort cells in the cortex of branches, *F. sericeum* has well-developed and typical retort-shaped cortical cells. It is currently ambiguous from our phylogenetic results whether the absence of retort cells in the *Ambuchanania* plus *Eosphagnum* clade represent a loss or plesiotypic absence. Our results are also ambiguous with regard to whether the absence of leaf cell fibrils in *F. sericeum* is derived or plesiotypic.

The positions and morphology of gametangia in *Ambuchanania* have weighed heavily in arguments that the species should be segregated from *Sphagnum* into its own genus, family, and order of Sphagnopsida (Crum and Seppelt, 1999; or in its own section of *Sphagnum*: Yamaguchi et al., 1990). The gametophytes are bisexual, but unlike bisexual species of *Sphagnum*, archegonia are terminal on the stems rather than on short lateral branches produced near the stem apices, and antheridia are borne at the bases of the perichaetia rather than on specialized branches of the capitula. Antheridia of *Ambuchanania* are elongate like



those found in other mosses, whereas antheridia are globose in all *Sphagnum* species from which they have been described (unknown in a few). The antheridia of *Flatbergium sericeum* are globose and therefore typically sphagnoid. The type specimen of *S. lapazense* bears no sporophytes or gametangia, but the type of *Eosphagnum inretortum* and the population from Chile had sporophytes when they were collected. Nevertheless, antheridia could not be located among plants from either locality. Most species of *Sphagnum* produce antheridia 6 months or more before they form mature sporophytes, so it is not surprising that both sporophytes and antheridia did not occur in the same collections. If it turns out that *E. inretortum* has typical round sphagnoid antheridia, it would imply that elongate antheridia is an autapomorphy for *Ambuchanania*. If on the other hand, *E. inretortum* has elongate antheridia, the evolution of this trait would remain ambiguous. The elongate antheridia of *Ambuchanania* might be a plesiomorphic trait retained from an ancestor in common with the Takakiopsida, or it could be a synapomorphy for the *Ambuchanania* plus *Eosphagnum* clade. The likelihood of these two alternative scenarios would depend on the relative branching order of Flatbergiaceae, Ambuchananiaceae, and Sphagnaceae.

**Timeframe of diversification in the Sphagnopsida**—Shaw et al. (2010) estimated divergence times from the phylogeny shown in Fig. 1 based on a relaxed clock model using Bayesian methods implemented in BEAST (Drummond and Rambaut, 2007), calibrated with estimated substitution rates of nuclear, plastid, and mitochondrial loci. Their estimates, albeit crude, suggest that the Sphagnopsida is an ancient group and diverged from the Takakiopsida between 129 and 319 million years ago (Ma), and the Flatbergiaceae plus Ambuchananiaceae diverged from the Sphagnaceae between 34 and 104 Ma. The diversification of extant *Sphagnum* species, in contrast, occurred relatively recently, between seven and 20 Ma, possibly associated with climatic cooling of the northern hemisphere and origin of boreal vegetation during the Miocene (Shaw et al., 2010).

The fossil record for *Sphagnum* and Sphagnopsida is very limited but what is known does not contradict this chronology. The earliest fossils attributed to the group belong to the Permian genus *Protosphagnum* (Neuberg, 1960). *Protosphagnum* is said to have a leaf midrib (unlike any extant *Sphagnum*), although the evidence based on photographs is not overly convincing. The species does appear to have dimorphic leaf cells. The arrangement of putative hyaline and chlorophyllose cells in *Protosphagnum* was interpreted by Butterfass (1992) in relation to the development of dimorphic cells in extant species, and it appears that the patterns of cell divisions may be similar. Actual developmental sequences for leaves of *Protosphagnum* are, of course, not known. A few other Paleozoic species of Sphagnopsida have been described but assigned to genera other than *Sphagnum*; leaves and spores that appear to represent *Sphagnum* are known from the Mesozoic and Tertiary (reviews in Lacey, 1969; Oostendorp, 1987).

If the divergence of *Ambuchanania* and *Eosphagnum* was some 50 Ma as implied by that chronology, it is perhaps less surprising that the two relictual species differ so greatly in morphology. The long branches separating early-diverging lineages within the Sphagnopsida (*Flatbergium*, *Ambuchanania*, *Eosphagnum*), and separating these lineages from *Sphagnum* s.s., suggest that extensive extinction of other early-diverging taxa might have occurred. By comparison, if we consider morphological diversity among extant species within

*Sphagnum* and imagine what levels of morphological disparity might look like if phylogenetically intermediate species were currently extinct, comparable patterns could occur. The morphological disparity between *E. inretortum* and *A. leucobryoides* could reflect extinction of other related species over the last ca. 50 Myr since the Ambuchananiaceae diverged from the Flatbergiaceae.

**Relationship of Sphagnopsida to other classes of phylum Bryophyta**—Several previous molecular analyses (e.g., Newton et al., 2000; Nickrent et al., 2000; Cox et al., 2004; Qiu et al., 2006) have resolved *Takakia* as sister to *Sphagnum*, though rarely with high bootstrap support. That sister-group relationship was also resolved by all analytical models we employed for the 60-taxon, eight-locus data set presented here. The ML and homogeneous Bayesian analyses provided strong support for a *Takakia* plus *Sphagnum* clade (95% and 91% bootstrap support in online Appendix S1, supplemental Figs. S.1.17 and S.1.18, 1.0 posterior probability in Fig. S.1.19). But when the polytomy prior was added to the Bayesian analysis (Fig. S.1.20) the posterior probability dropped to 0.92, and when composition was modeled across the tree (Appendix S1: Figs. S.1.21, S.1.22—S.1.28), support disappeared completely. These results suggest that support for the *Takakia* plus Sphagnopsida clade may be due to a phylogenetic artifact caused by nonstationary composition bias.

Morphological characters suggest a closer relationship of *Takakia* to *Andreaea* and/or *Andreaebryum* than to *Sphagnum* (Murray, 1988; Renzaglia et al., 1997). However, at least some such similarities may be plesiotypic within the mosses (for example, effects [or lack thereof] of calyptrae on normal capsule development, restriction of placental transfer cells to the sporophyte tissue, absence of sporophytic conducting cells [Renzaglia et al., 1997]) and are therefore uninformative with regard to relationships among groups. A critical feature is the embryological origins of the sporogenous tissue of sporophytes derived from the endothecium in *Andreaea*, *Andreaebryum*, and bryopsid mosses, but from the amphithecium in *Sphagnum*. Origin of the sporogenous tissue in *Takakia* is not known, though anatomical features of mature sporophytes suggest that it may be endothecial.

Overall, *Takakia* and species of *Sphagnopsida* are extremely different in morphology, but *Takakia* is also very different from *Andreaea*, *Andreaebryum*, or any other moss. If phylogenetic reconstructions that resolve Sphagnopsida plus *Takakia* as sister to a clade containing *Andreaea*, *Andreaebryum*, and the rest of the (bryopsid) mosses, a classification of phylum Bryophyta with two subphyla would best reflect history. This would provide an alternative hypothesis to that of Stech and Frey (2008) in which three groups of equal rank are recognized (Takakiophytina, Sphagnophytina, Bryophytina), or that of Goffinet et al. (2009) in which five groups are distinguished (Sphagnopsida, Takakiopsida, Andreaebryopsida, Andreaeopsida, Bryopsida).

#### LITERATURE CITED

- ANDREWS, A. L. 1911. Notes on North American *Sphagnum*. I. The groups. *Bryologist* 14: 72–75.
- BECKERT, S., S. STEINHAUSER, H. MUHLE, AND V. KNOOP. 1999. A molecular phylogeny of the bryophytes based on nucleotide sequences of the mitochondrial *nad5* gene. *Plant Systematics and Evolution* 218: 179–192.
- BENNETT, M. D., AND I. J. LEITCH. 2005. Plant DNA C-values database (release 4.0, October 2005). Website <http://data.kew.org/cvalues/>.

- BOLLBACK, J. P. 2002. Bayesian model adequacy and choice in phylogenetics. *Molecular Biology and Evolution* 19: 1171–1180.
- BOWER, F. O. 1935. Primitive land plants. Macmillan, London, UK.
- BUTTERFASS, T. 1992. The patterns of cell division and chloroplast reproduction in young leaflets of *Sphagnum*. *Journal of Bryology* 17: 143–153.
- CAMPBELL, D. H. 1895. The structure and development of mosses and ferns (Archegoniatae). Macmillan and Co., London, UK.
- CAVERS, F. 1911. The inter-relationships of the Bryophyta. *New Phytologist* reprint 4. Botany School, Cambridge, UK.
- COX, C. J., P. G. FOSTER, R. P. HIRT, S. R. HARRIS, AND M. T. EMBLEY. 2008. The archaeobacterial origins of eukaryotes. *Proceedings of the National Academy of Sciences, USA* 105: 20356–20361.
- COX, C. J., B. GOFFINET, A. E. NEWTON, A. J. SHAW, AND T. A. J. HEDDERSON. 2000. Phylogenetic relationships among the diplolepidoid-alternate mosses (Bryidae) inferred from nuclear and chloroplast DNA sequences. *The Bryologist* 103: 224–240.
- COX, C. J., B. GOFFINET, A. J. SHAW, AND S. BOLES. 2004. Phylogenetic relationships among the mosses based on heterogeneous Bayesian analysis of multiple genes from multiple genomic compartments. *Systematic Botany* 29: 234–250.
- COX, C. J., AND T. A. J. HEDDERSON. 1999. Phylogenetic relationships among the ciliate arthroodontous mosses: Evidence from chloroplast and nuclear DNA sequences. *Plant Systematics and Evolution* 215: 119–139.
- CROSBY, M. R., R. E. MAGILL, B. ALLEN, AND S. HE. 2000. A checklist of the mosses. Missouri Botanical Garden, St. Louis, Missouri, USA. Website <http://www.mobot.org/MOBOT/tropicos/most/checklist.shtml>.
- CRUM, H. A. 1984. Sphagnopsida, Sphagnaceae. North American Flora, series 2, part 11, 1–180. New York Botanical Garden, New York, New York, USA.
- CRUM, H. A. 1990. *Sphagnum inretortum*, a new species in a new section from Bolivia. *Bryologist* 93: 283–285.
- CRUM, H. A. 1992. Miscellaneous notes on the genus *Sphagnum*. 1–2. *Bryologist* 95: 274–279.
- CRUM, H. A. 2001a. Miscellaneous notes on *Sphagnum*—11. *Contributions from the University of Michigan Herbarium* 23: 107–114.
- CRUM, H. A. 2001b. Structural diversity of bryophytes. University of Michigan Herbarium, Ann Arbor, Michigan, USA.
- CRUM, H. A., AND R. D. SEPPELT. 1999. *Sphagnum leucobryoides* reconsidered. *Contributions from the University of Michigan Herbarium* 22: 29–31.
- DOLEŽEL, J., J. BARTOŠ, H. VOGLMAYR, AND J. GREILHUBER. 2003. Nuclear DNA content and genome size of trout and human. *Cytometry* 51A: 127–128.
- DRUMMOND, A. J., AND A. RAMBAUT. 2007. BEAST: Bayesian evolutionary analysis by sampling trees. *BMC Evolutionary Biology* 7: 214.
- DUCKETT, J. G., S. PRESSEL, K. N. Y. P'NG, AND K. S. RENZAGLIA. 2009. Exploding a myth: The capsule dehiscence mechanism and function of pseudostomata in *Sphagnum*. *New Phytologist* 183: 1053–1063.
- EDDY, A. 1977. Sphagnales of tropical Asia. *Bulletin of the British Museum (Natural History). Historical Series* 5: 359–445.
- EDGAR, R. C. 2004. MUSCLE: Multiple sequence alignment with high accuracy and high throughput. *Nucleic Acids Research* 32: 1792–1797.
- FLEISCHER, M. 1923. Allgemeine Uebersicht des natürlichen Systems der Laubmoose. In *Die Moose der Flora von Buitenzorg* 4: XI–XXIII. E. J. Brill, Leiden, Netherlands.
- FOSTER, P. 2004. Modeling compositional heterogeneity. *Systematic Biology* 53: 485–495.
- FRITSCH, R. 1982. Index to plant chromosome numbers—Bryophyta. Scheltema and Holkema, Boston, Massachusetts, USA.
- GALTIER, N., M. GOUY, AND C. GAUTIER. 1996. SEA VIEW and PHYLO-WIN: Two graphic tools for sequence alignment and molecular phylogeny. *CABIOS* 12: 543–548.
- GARBARY, D. J., K. S. RENZAGLIA, AND J. G. DUCKETT. 1993. The phylogeny of land plants: A cladistic analysis based on male gametogenesis. *Plant Systematics and Evolution* 188: 237–269.
- GOFFINET, B., W. R. BUCK, AND A. J. SHAW. 2009. Morphology, anatomy, and classification of the Bryophyta. In B. Goffinet and A. J. Shaw [eds.], *Bryophyte biology*, 2nd ed., 55–138. Cambridge University Press, New York, New York, USA.
- GOFFINET, B., C. J. COX, A. J. SHAW, AND T. A. J. HEDDERSON. 2001. The Bryophyta (mosses): Systematic and evolutionary inferences from an *rps4* gene (cpDNA) phylogeny. *Annals of Botany* 87: 191–208.
- GREILHUBER, J., AND I. EBERT. 1994. Genome size variation in *Pisum sativum*. *Genome* 37: 646–655.
- HAECKEL, E. 1876. The history of creation, vol. 2., Appelton, New York, New York, USA.
- HEDDERSON, T. A., R. L. CHAPMAN, AND W. L. ROOTES. 1996. Phylogenetic relationships of bryophytes inferred from nuclear encoded rRNA gene sequences. *Plant Systematics and Evolution* 200: 213–224.
- HOLCOMBE, J. W. 1984. Morphogenesis of branch leaves of *Sphagnum magellanicum* Brid. *Journal of the Hattori Botanical Laboratory* 57: 179–240.
- ISOVIITA, P. 1966. Studies on *Sphagnum* L. 1. Nomenclatural revision of the European taxa. *Annales Botanici Fennici* 3: 199–264.
- JOHNSON, K. A., J. WHINAM, A. M. BUCHANAN, AND J. BALMER. 2008. Ecological observations and new locations of a rare moss, *Ambuchania leucobryoides*. *Papers and Proceedings of the Royal Society of Tasmania* 142: 79–84.
- KARLIN, E. F., S. B. BOLES, M. RICCA, E. M. TEMSCH, J. GREILHUBER, AND A. J. SHAW. 2009. Three genome mosses: Complex double allopolyploid origins for triploid gametophytes in *Sphagnum*. *Molecular Ecology* 18: 1439–1454.
- KENRICK, P., AND P. R. CRANE. 1997. The origin and early diversification of land plants: A cladistic study. Smithsonian Institution Press, Washington, D.C., USA.
- LACEY, W. S. 1969. Fossil bryophytes. *Biological Reviews of the Cambridge Philosophical Society* 44: 189–205.
- LARTILLOT, N., AND H. A. PHILIPPE. 2004. Bayesian mixture model for across-site heterogeneities in the amino-acid replacement process. *Molecular Biology and Evolution* 21: 1095–1109.
- LEWIS, P. O., M. HOLDER, AND K. E. HOLSINGER. 2005. Polytomies and Bayesian phylogenetic inference. *Systematic Biology* 54: 241–253.
- LI, X.-J., AND S. HE. 1999. Sphagnaceae. In C. Chen, M. R. Crosby, and S. He [eds.], *Moss flora of China*, vol. 1, 3–48. Missouri Botanical Garden, St. Louis, Missouri, USA.
- LIGRONE, R., AND J. G. DUCKETT. 1998. Development of the leafy shoot in *Sphagnum* (Bryophyta) involves the activity of both apical and sub-apical meristems. *New Phytologist* 140: 581–595.
- LIGRONE, R., J. G. DUCKETT, AND K. S. RENZAGLIA. 1993. The gametophyte-sporophyte junction in land plants. *Advances in Botanical Research* 19: 231–317.
- LINDBERG, S. O. 1882. Europas och Nord Amerikas hvitmossor (sphagna). J. C. Frenckell, Helsinki, Finland.
- MISHLER, B. D., AND S. P. CHURCHILL. 1984. A cladistic approach to the phylogeny of the “bryophytes”. *Brittonia* 36: 406–424.
- MURRAY, B. M. 1988. Systematics of the Andreaeopsida (Bryophyta): Two orders with links to *Takakia*. *Beihefte zur Nova Hedwigia* 90: 289–336.
- NEUBERG, M. F. 1960. Leafy mosses from the Permian deposits of Angarida. *Trudy Geological Institute, Leningrad* 19: 1–104 [in Russian].
- NEWTON, A. E., C. J. COX, J. G. DUCKETT, J. A. WHEELER, B. GOFFINET, T. A. J. HEDDERSON, AND B. D. WHEELER. 2000. Evolution of the major moss lineages: Analyses based on multiple genes sequences and morphology. *Bryologist* 103: 187–211.
- NEWTON, M. A., AND A. E. RAFTERY. 1994. Approximate Bayesian inference with the weighted likelihood bootstrap. *Journal of the Royal Statistical Society, B, Methodological* 56: 3–48.
- NICKRENT, D. L., C. L. PARKINSON, J. D. PALMER, AND R. J. DUFF. 2000. Multigene phylogeny of land plants with special reference to bryophytes and the earliest land plants. *Molecular Biology and Evolution* 17: 1885–1895.
- NISHIYAMA, T., P. G. WOLF, M. KUGITA, R. B. SINCLAIR, M. SUGITA, C. SUGIURA, T. WAKASUGI, ET AL. 2004. Chloroplast phylogeny indicates that bryophytes are monophyletic. *Molecular Biology and Evolution* 21: 1813–1819.

- NYLANDER, J. A. A. 2004. MrModeltest v2. Program distributed by the author. Evolutionary Biology Centre, Uppsala University, Uppsala, Sweden.
- OOSTENDORP, C. 1987. The bryophytes of the Palaeozoic and the Mesozoic. *Bryophytorum Bibliotheca* 34. J. Cramer, Berlin, Germany.
- QIU, Y.-L., Y. CHO, J. C. COX, AND J. D. PALMER. 1998. The gain of three mitochondrial introns identifies liverworts as the earliest land plants. *Nature* 394: 671–674.
- QIU, Y.-L., L. LI, B. WANG, Z. CHEN, V. KNOOP, M. GROTH-MALONEK, O. DOMBROVSKA, ET AL. 2006. The deepest divergences in land plants inferred from phylogenomic evidence. *Proceedings of the National Academy of Sciences, USA* 103: 15511–15516.
- RENZAGLIA, K. S., K. D. MCFARLAND, AND D. K. SMITH. 1997. Anatomy and ultrastructure of the sporophyte of *Takakia ceratophylla* (Bryophyta). *American Journal of Botany* 84: 1337–1350.
- RICCA, M., F. W. BEECHER, S. B. BOLES, E. TEMSCH, J. GREILHUBER, E. KARLIN, AND A. J. SHAW. 2008. Cytotype variation and allopolyploidy in North American species of the *Sphagnum subsecundum* complex. *American Journal of Botany* 95: 1606–1620.
- RODRÍGUEZ-EZPELETA, N., H. PHILIPPE, H. BRINKMANN, B. BECKER, AND M. MELKONIAN. 2007. Phylogenetic analyses of nuclear, mitochondrial, and plastid multigene data sets support the placement of Mesostigma in the Streptophyta. *Molecular Biology and Evolution* 24: 723–731.
- RONQUIST, F., AND J. P. HUELSENBECK. 2003. MrBayes 3: Bayesian phylogenetic inference under mixed models. *Bioinformatics* 19: 1572–1574.
- SCHOFIELD, W. B. 1985. Introduction to bryology. Macmillan, New York, New York, USA.
- SEPPELT, R. D. 2000. The Sphagnopsida (Sphagnaceae; Ambuchananiaceae) in Australia. *Hikobia* 13: 163–183.
- SHAW, A. J., C. J. COX, AND S. B. BOLES. 2005. Phylogeny, species delimitation, and interspecific hybridization in *Sphagnum* section *Acutifolia*. *Systematic Botany* 30: 16–33.
- SHAW, A. J., N. DEVOS, C. J. COX, S. B. BOLES, B. SHAW, A. M. BUCHANAN, L. CAVE, AND R. SEPPELT. 2010. Peatmoss (*Sphagnum*) diversification associated with Miocene Northern Hemisphere climatic cooling? *Molecular Phylogenetics and Evolution* 55: 1139–1145.
- SHAW, A. J., AND K. S. RENZAGLIA. 2004. Phylogeny and diversification of bryophytes. *American Journal of Botany* 91: 1557–1581.
- SHAW, J. 2000. Phylogeny of the Sphagnopsida based on nuclear and chloroplast DNA sequences. *Bryologist* 103: 277–306.
- SHAW, J., C. J. COX, AND S. B. BOLES. 2003. Polarity of peatmoss (*Sphagnum*) evolution: Who says mosses have no roots? *American Journal of Botany* 90: 1777–1787.
- SHAW, S., C. J. COX, AND S. B. BOLES. 2004. Phylogenetic relationships among *Sphagnum* sections, *Hemitheca*, *Isocladus*, and *Subsecunda*. *Bryologist* 107: 189–196.
- STAMATAKIS, A. 2006. RAXML-VI-HPC: Maximum likelihood-based phylogenetic analyses with thousands of taxa and mixed models. *Bioinformatics* 22: 2688–2690.
- STAMATAKIS, A., P. HOOVER, AND J. ROUGEMONT. 2008. A rapid bootstrap algorithm for the RAXML web servers. *Systematic Biology* 57: 758–771.
- STECH, M., AND W. FREY. 2008. A morpho-molecular classification of the mosses (Bryophyta). *Nova Hedwigia* 86: 1–21.
- STEERE, W. C. 1958. Evolution and speciation in mosses. *American Naturalist* 92: 5–20.
- SWOFFORD, D. L. 1998. PAUP\*: Phylogenetic analysis using parsimony (\*and other methods). Sinauer, Sunderland, Massachusetts, USA.
- TEMSCH, E. M., J. GREILHUBER, AND R. KRISAI. 1998. Genome size in *Sphagnum* (peat moss). *Botanica Acta* 111: 325–330.
- TEMSCH, E. M., J. GREILHUBER, AND R. KRISAI. 2010. Genome size in liverworts. *Preslia* 82: 63–80.
- TERASAWA, K., M. ODAHARA, Y. KABEYA, T. KIKUGAWA, Y. SEKINE, M. FUJIWARA, AND N. SATO. 2007. The mitochondrial genome of the moss *Physcomitrella patens* sheds new light on mitochondrial evolution in land plants. *Molecular Biology and Evolution* 24: 699–709.
- VANDERPOORTEN, A., AND B. GOFFINET. 2009. Introduction to bryophytes. Cambridge University Press, Cambridge, UK.
- VITT, D. H. 1984. Classification of the Bryopsida. In R. M. Schuster [ed.], New manual of bryology, vol. 2, 676–759. Hattori Botanical Laboratory, Nichinan, Japan.
- VOGLMAYR, H. 2000. Nuclear DNA amounts in mosses (Musci). *Annals of Botany* 85: 531–546.
- WAHRMUND, U., D. QUANDT, AND V. KNOOP. 2010. The phylogeny of mosses—addressing open issues with a new mitochondrial locus: group I intron cob1420. *Molecular Phylogenetics and Evolution* 54: 417–426.
- WARNSTORF, C. 1911. Sphagnales-Sphagnaceae (Sphagnologia Universalis). In H. G. A. Engler [ed.], Das Pflanzenreich, Heft 51. Engelmann, Leipzig, Germany.
- YAMAGUCHI, T., R. D. SEPPELT, Z. IWATSUKI, AND A. M. BUCHANAN. 1990. *Sphagnum* (section *Buchanania*) *leucobryoides* sect. et sp. nov. from Tasmania. *Journal of Bryology* 16: 45–64.

APPENDIX 1. Accession information and GenBank numbers for samples included in phylogenetic analyses of the Sphagnopsida. A dash (—) means a sequence was not obtained. Herbarium acronyms: DUKE = Duke University, MICH = University of Michigan, NY = New York Botanical Garden, RNG = University of Reading.

**Taxon;** Isolate number; GenBank accessions: *rps4*, *trnL*, *psbA*, *nuc18S*, *nuc26S-1*, *nuc26S-2*, *rbcL*, *nad5*, *nad7*, *trnG*; *Voucher specimen*, Herbarium.

- Alophosia azorica* (Renauld & Cardot) Cardot; MDP332; AY330476, —, AY312891, —, AY330424, GQ368591, AY312924, AY312867, AY330453, GQ368647; *Rumsey s.n.*; DUKE. *Ambuchanania leucobryoides* Seppelt & H.A. Crum; SB3269; GQ368612, GQ368649, GQ368606, GQ375079, GQ375083, GQ368584, GQ368609, GQ368600, GQ368603, GQ368615; *Buchanan s.n.*; DUKE. *Andreaea wilsonii* Hook. f.; B75; AY330477, AY312939, AY312892, AY330416, AY330425, —, AY312925, AY312868, AY330454, —; *Cox 00-668*; DUKE. *Andreaebryum macrosporum* Steere & B. M. Murray; SB472; AF3306953, —, AY312893, AJ275005, AY330426, —, AF231059, —, —; *Schofield 78094*; DUKE. *Aulacomnium turgidum* (Wahlenberg) Schwägr.; A37; AF023809, AF023728, AY312894, AF023687, AY330427, —, AJ275180, AY312869, AY330455, —; *Hedderson 6385*; RNG. *Bartramia stricta* Brid.; E3; AF023799, AF023756, AY312895, AF023698, AY330428, GQ368570, AY312926, AY312870, AY330456, GQ368645; *Longton 4871*; RNG. *Brachythecium salebrosum* (Hoffm. ex F. Weber & D. Mohr) Schimp.; BB86; AF143027, AF161120, AY312896, AY330417, AY330429, GQ368571, AY312927, AY312871, AY330457, GQ368646; *Goffinet 4723*; NY. *Buxbaumia aphylla* Hedw.; B759; AF3306959, AF231909, AY312897, Y17603, AY330430, GQ368572, GQ368610, AY312872, —, GQ368643; *Belland 16889*; DUKE. *Dendrologotrichum dendroides* (Brid. ex Hedw.) Broth.; BG977; AF208420, AY312940, AY312898, AY330418, AY330431, GQ368573, AF208411, AY312873, AY330458, GQ368644; *Goffinet 5425*; DUKE. *Diphyscium foliosum* (Hedw.) D. Mohr; BG712; AJ251065, AF229891, AY312899, Y17765, AY330432, AF023799, AF023756, AY312895, AF023698, AY330428, GQ368570, AY312926, AY312870, AY330456, GQ368645; *Longton 4871*; RNG. *Encalypta ciliata* Hedw.; BG713; AF223040, AF229897, AY312900, AF223011, AY330433, GQ368575, AY312929, AY312875, AY330460, GQ368641; *Schofield 98872*; DUKE. *Entosthodon laevis* (Mitt.) Fife; BG980; AY330478, AY312941, AY312901, AY330419, AY330434, GQ368580, AY312930, AY312876, AY330461, GQ368639; *Goffinet 5601*; DUKE. *Fissidens subbasilaris* Hedw.; BG984; AF223056, AF229913, AY312902, AF223027, AY330435, GQ368581, AF231304, AY312877, AY330462, GQ368640; *Goffinet 5263*; DUKE. *Funaria hygrometrica* Hedw.; C148; AF023776, AF231175, AY312903, X74114, AY330436, GQ368582, AF005513, Z98959, AY330463, GQ368636; *Cox 148*; RNG. *Haplomitrium hookeri* (Sm.) Nees; SB475; AJ251064, AY312942, AY312904, Y19006, AY330437, GQ368583, U87072, AY608284, —, GQ368637; *Schofield 95224*; DUKE. *Hedwigia ciliata* (Hedw.) P. Beauv.; A31; AJ251309, AF233587, AY312905, AJ275010, AY330438, —, AF231073, Z98966, AY330464, GQ368638; *Hedderson 11771*; RNG. *Hookeria lucens* (Hedw.) Smith; A80; AJ251316, AF215906, AY312906, AJ243168, AY330439, GQ368588, AY312931, Z98969, AY330465, GQ368635; *Cox 118*; RNG. *Leucobryum sp.*; AV\_G7; GQ368613, GQ368650, GQ368607, —, GQ375084, GQ368585, —, GQ368601, GQ368604, GQ368617; *Vanderpoorten s.n.*; DUKE. *Mielichhoferia elongata* (Hoppe & Hornsch.) Nees & Hornsch.; SH5; AF023793, AF023766, AY312907, AF023708, AY330440, —, AF232693, AY312878, —, GQ368634; *Shaw s.n.*; RNG. *Mnium hornum* Hedw.; C115; AF023796, AF182360, AY312908, X80985, AY330441, GQ368586, AF226820, AY312879, —, GQ368632; *Cox 115*; RNG. *Oedipodium griffithianum* (Dicks.) Schwägr.; BG656; AF306968, AF246290, AY312909, AF228668, AY330442, GQ368576, AY312932, AY312880, AY330466, GQ368633; *Schofield 98670*; DUKE. *Orthodontium lineare* Schwägr.; A79; AF023800, AF023768, AY312910, AF023697, AY330443, GQ368577, AJ275174, AY312881, AY330467, GQ368629; *Hedderson s.n.*; RNG. *Orthotrichum lyelli* Hook. & Taylor; L16; AF023814, AF023727, AY312911, AF025291, AY330444, GQ368578, AF005536, AY312882, AY330468, GQ368630; *Hedderson 5745*; RNG. *Pellia epiphylla* (L.) Corda; B97; AY330479, —, AY312912, X80210, AF226030, —, U87085, AY608305, —, GQ368631; *Risk & Gross 12231*; DUKE. *Polytrichadelphus purpureus* Mitt.; MDP353; AY330480, AY312943, AY312913, AY330420, —, GQ368587, AY312933, AY312883, AY330469, GQ368626; *Cox 84/01*; DUKE. *Polytrichum pallidisetum* Funck; BG768; AF306956, AY312944, AY312914, AY330421, AY330445, GQ368579, AY312934, AY312884, AY330470, GQ368625; *Goffinet 4581*; DUKE. *Porella pinnata* L.; BG1072; AY330481, AY312945, AY312915, AY330422, AY330446, GQ368592, U87088, AY608308, —, GQ368627; *Goffinet 4744*; DUKE. *Preissia quadrata* (Scop.) Nees; BG1080; AY330482, AY312946, AY312916, X80211, AY330447, GQ368589, AY312935, AY608309, —, GQ368628; *Schofield 105579*; DUKE. *Pyrrhobryum vallis-gratae* (Hampe ex Müll. Hal.) Manuel; 11755; AF023825, AF023754, AY312917, AF023695, AY330448, GQ368593, AJ275179, AY312885, AY330471, GQ368620; *Hedderson 11775*; RNG. *Rhodobryum giganteum* (Schwägr.) Paris; 5073; AF023789, AF023737, AY312918, AF023699, AY330449, GQ368590, AJ275176, AY312886, —, GQ368621; *Longton 5073*; RNG. *Scouleria aquatica* Hook.; 5811; AF023780, AF023723, AY312919, AF023684, AY330450, GQ368599, AF226822, AY312887, AY330472, GQ368622; *Hedderson 5811*; RNG. *Sphagnum affine* Renauld & Cardot; SB1211; AY309713, AY297996, AY309603, —, AY309504, AY313205, AY309689, AY309555, AY309579, AY309755; *Long 28884*; DUKE. *Sphagnum angustifolium* (Warnst.) C.E.O. Jensen; SB542; AY309714, AY298005, AY309604, GQ375058, AF197086, AF198021, AY309690, AY309556, AY309580, AY309756; *Shaw 9639*; DUKE. *Sphagnum aongstroemii* C. Hartman; SB412; AY309715, AF192619, AY309605, GQ375074, AF197083, AF198018, AY309691, AY309557, AY309581, AY309757; *Andrus & Flatberg 7531*; DUKE. *Sphagnum compactum* Lam. & DC.; SB80; AY309716, AF192578, AY309606, GQ375073, AF197069, AF198004, AY309696, AY309558, AY309582, AY309758; *Shaw 9332*; DUKE. *Sphagnum cuspidatum* Ehrh. ex Hoffm.; SB642; AY309718, AF192633, AY309608, GQ375066, AY309506, AY313206, AY309694, AY309560, AY309584, AY309760; *Shaw 9327*; DUKE. *Sphagnum cyclophyllum* Sull. & Lesq.; SB78; AY309719, AF192562, AY309609, GQ375063, AF197067, AF198002, AY309695, AY309561, AY309585, AY309761; *Shaw 8560*; DUKE. *Sphagnum cymbifolioides* Breutel; SB127; AY309720, AF192584, AY309610, GQ375064, AF197076, AF198011, AY309696, AY309562, AY309586, AY309762; *Streimann 47192*; NY. *Sphagnum fuscum* (Schimp.) H. Klinggr.; SB571; AY309721, AY347095, AY309611, GQ375070, AF197091, AF198026, AY309697, AY309563, AY309587, AY309763; *Shaw 9678*; DUKE. *Sphagnum inretortum* H.A. Crum; SB1052; AY309722, AY298153, AY309612, GQ375081, AY309507, —, AY309698, AY309564, AY309588, AY309764; *Price et al. 1236 Bolivia*; MICH. *Sphagnum inretortum* H.A. Crum; SB3274; GQ368614, GQ368651, GQ368608, GQ375082, —, —, GQ368611, GQ368602, GQ368605, GQ368648; *Andrus 11835 Chile*; DUKE. *Sphagnum lescurei* Sull.; SB77; AY309723, AF192565, AY309613, GQ375069, AF197066, AF198001, AY309699, AY309565, AY309589, AY309765; *Shaw s.n.*; DUKE. *Sphagnum palustre* L.; SB1209; AF231882, AF192634, AY312920, Y11370, AY330451, GQ368594, AF231887, AY312888, AY330473, GQ368623; *Long 28667*; DUKE. *Sphagnum perichaetiale* Hampe; SB74; AY309724, AF192575, AY309614, GQ375078, —, AF197999, AY309700, AY309566, AY309590, AY309766; *Shaw 9213*; DUKE. *Sphagnum portoricense* Hampe; SB106; AY309725, AF192577, AY309615, GQ375062, AF197077, AF198012, AY309701, AY309567, AY309591, AY309767; *Anderson 26770*; DUKE. *Sphagnum pulchrum* (Lindb.) Warnst.; SB543; AY309726, AY298224, AY309616, GQ375067, AF197087, AF198022, AY309702, AY309568, AY309592, AY309768; *Shaw 9796*; DUKE. *Sphagnum quinquefarium* (Lindb.) Warnst.; SB576; AY309727, AF192608, AY309617, GQ375061, AF197089, AF198024, AY309703, AY309569, AY309593, AY309769; *Shaw 9682*; DUKE. *Sphagnum recurvum* P. Beauv.; SB83; AY309728, AF192569, AY309618, GQ375065, AF197072, AF198007, AY309704, AY309570, AY309594, AY309770; *Shaw 9196*; DUKE. *Sphagnum sericeum* Müll. Hal. 1; SB858; AY309717, AY298061, AY309607, GQ375072, AY309505, —, AY309693, AY309559, AY309583, AY309759; *Tan & Harrison s.n.*; DUKE. *Sphagnum sericeum* Müll. Hal. 2; SB1239; AY309729, AY298280, AY309619, GQ375071, AY309508, AY313207, AY309705, AY309571, AY309595, AY309771; *Yamaguchi*

18926; DUKE. *Sphagnum squarrosum* Crome; SB1248; AY309730, AY298287, AY309620, GQ375075, AY309509, AY313208, AY309706, AY309572, AY309596, AY309772; *Higuchi 40888*; DUKE. *Sphagnum steerei* R.E. Andrus; SB367; AY309731, AF192574, AY309621, GQ375077, AF197081, AF198016, AY309707, AY309573, AY309597, AY309773; *Andrus 8574*; DUKE. *Sphagnum strictum* Sull.; SB79; AY309732, AF192585, AY309622, GQ375080, AF197068, AF198003, AY309708, AY309574, AY309598, AY309774; *Shaw 9406*; DUKE. *Sphagnum subnitens* Russow & Warnst.; SB538; AY309733, AY298303, AY309623, GQ375059, AF197092, AF198027, AY309709, AY309575, AY309599, AY309775; *Shaw 9723*; DUKE. *Sphagnum tenerum* Sull. & Lesq. ex Sull.; SB75; AY309734, AF192588, AY309624, GQ375060, AF197065, AF198000, AY309710, AY309576, AY309600, AY309776; *Shaw 9335*; DUKE. *Sphagnum teres* (Schimp.) Ångström; SB366; AY309735, AF192596, AY309625, GQ375076, AF197090, AF198025,

AY309711, AY309577, AY309601, AY309777; *Hedderson 7928*; DUKE. *Sphagnum wulfianum* Girgensohn; SB1288; AY309736, AY298357, AY309626, GQ375068, AY309510, AY313209, AY309712, AY309578, AY309602, AY309778; *Shaw 9855*; DUKE. *Takakia lepidozoides* S. Hatt. & H. Inoue; SB473; AF306950, AY312947, AY312921, AJ269686, AF197061, GQ368598, AY312936, AY312889, AJ309978, GQ368624; *Schofield 86563*; DUKE. *Tetraxis pellucida* Hedw.; MDP474; AY908021, AF231908, —, U18527, AF226033, GQ368596, U87091, AY908812, —, GQ368619; *Risk & Gross 105858*; DUKE. *Tetraplodon mnioides* (Sw. ex Hedw.) Bruch & Schimp.; L3; AF023804, AF023730, AY312922, AF023691, —, GQ368595, AY312937, —, AY330474, GQ368618; *Soderstrom s.n.*; RNG. *Timmia megapolitana* Hedw.; BG1003; AF222902, AY312948, AY312923, AY330423, AY330452, GQ368597, AY312938, AY312890, AY330475, GQ368616; *Schofield 97957*; DUKE.

---